JOURNAL OF VIROLOGY, Nov. 2008, p. 10998–11008 Vol. 82, No. 22
0022-538X/08/$08.00+0 doi:10.1128/JVI.01311-08

Mouse APOBEC3 Restricts Friend Leukemia Virus Infection and Pathogenesis In Vivo▽

Eri Takeda,[1] Sachiyo Tsuji-Kawahara,[1] Mayumi Sakamoto,[1] Marc-André Langlois,[2] Michael S. Neuberger,[2] Cristina Rada,[2] and Masaaki Miyazawa[1]*

Department of Immunology, Kinki University School of Medicine, 377-2 Ohno-Higashi, Osaka-Sayama, Osaka 589-8511, Japan,[1] and Medical Research Council, Laboratory of Molecular Biology, Hills Road, Cambridge CB2 2QH, United Kingdom[2]

Received 24 June 2008/Accepted 3 September 2008

Several members of the apolipoprotein B mRNA-editing enzyme catalytic polypeptide-like complex 3 (APOBEC3) family in primates act as potent inhibitors of retroviral replication. However, lentiviruses have evolved mechanisms to specifically evade host APOBEC3. Likewise, murine leukemia viruses (MuLV) exclude mouse APOBEC3 from the virions and cleave virion-incorporated APOBEC3. Although the betaretrovirus mouse mammary tumor virus has been shown to be susceptible to mouse APOBEC3, it is not known if APOBEC3 has a physiological role in restricting more widely distributed and long-coevolved mouse gammaretroviruses. The pathogenicity of Friend MuLV (F-MuLV) is influenced by several host genes: some directly restrict the cell entry or integration of the virus, while others influence the host immune responses. Among the latter, the *Rfv3* gene has been mapped to chromosome 15 in the vicinity of the *APOBEC3* locus. Here we have shown that polymorphisms at the mouse *APOBEC3* locus indeed influence F-MuLV replication and pathogenesis: the *APOBEC3* alleles of F-MuLV-resistant C57BL/6 and -susceptible BALB/c mice differ in their sequences and expression levels in the hematopoietic tissues and in their abilities to restrict F-MuLV replication both in vitro and in vivo. Furthermore, upon infection with the pathogenic Friend virus complex, (BALB/c × C57BL/6)F_1 mice displayed an exacerbated erythroid cell proliferation when the mice carried a targeted disruption of the C57BL/6-derived *APOBEC3* allele. These results indicate, for the first time, that mouse APOBEC3 is a physiologically functioning restriction factor to mouse gammaretroviruses.

The apolipoprotein B mRNA-editing enzyme catalytic polypeptide-like editing complex 3 (APOBEC3) proteins are cellular cytidine deaminases with potent antiretroviral activities (reviewed in reference 8). Thus, after the penetration of retroviral nucleocapsids into target cells of infection and the initiation of reverse transcription, APOBEC3 enzymes can induce the conversion of cytosine to uracil in the minus-sense single-strand viral DNA, leading to G-to-A hypermutations in the subsequent plus-strand viral DNA. The resultant detrimental levels of mutations in the proviral genome, along with a deamination-independent mechanism that works prior to the proviral integration (9), together exert efficient antiretroviral effects in infected target cells. However, retroviruses have evolved to evade their natural hosts' APOBEC3. Thus, human immunodeficiency virus (HIV) counters the action of human APOBEC3G (hAPOBEC3G) through its viral infectivity factor (Vif). The Vif protein expressed in virus-producing cells interacts with hAPOBEC3G to recruit ubiquitin ligase complex and thus mediates polyubiquitination of hAPOBEC3G and Vif, resulting in rapid degradation of hAPOBEC3G (11, 29, 49). Vif is also known to partially impair de novo synthesis of hAPOBEC3G (45). Therefore, hAPOBEC3G is neutralized by HIV Vif, as well as simian immunodeficiency virus (SIV) Vif from the chimpanzee, rhesus macaque, and sooty mangabey (28). However, the antiretroviral effects of human APOBEC3 (hAPOBEC3) proteins are not limited to Vif-deficient lentiviruses of the above-mentioned primate species but are readily exerted with other lentiviruses including SIV from the African green monkey, equine infectious anemia virus, and more distantly related retroviruses such as murine leukemia virus (MuLV), porcine endogenous retrovirus, and foamy viruses (12, 16, 21, 27). The hAPOBEC3G has also been shown to restrict retrotransposition of Alu elements (10), indicating a possible physiological role for APOBEC3 proteins in protecting cells from endogenous retroelements.

Similarly, mouse APOBEC3 (mAPOBEC3) restricts the replication of HIV type 1 (HIV-1) without being countered by Vif (28, 42), whereas mouse gammaretroviruses are relatively resistant to mAPOBEC3 (1, 4, 13). This resistance of mouse gammaretroviruses to the APOBEC3 protein of their natural host seems to be mediated through the exclusion of mAPO BEC3 from MuLV particles and cleavage of virion-incorporated mAPOBEC3 by the viral protease (1, 4, 13). Interestingly, however, mouse mammary tumor virus (MMTV), a betaretrovirus, is susceptible to mAPOBEC3 (39), and evidence has been shown that endogenous polytropic and modified polytropic retroviruses have been genetically modified through the action of mAPOBEC3 (19). Thus, increasing evidence indicates a possible physiological role for mAPOBEC3 in restricting the replication of gammaretroviruses, not just betaretroviruses, of cognate origin; however, direct demonstration of the protective effects exerted by mAPOBEC3 on pathogenic MuLV infection has been lacking (4).

Friend virus (FV) is the pathogenic retrovirus complex composed of replication-competent Friend MuLV (F-MuLV), a

* Corresponding author. Mailing address: Department of Immunology, Kinki University School of Medicine, 377-2 Ohno-Higashi, Osaka-Sayama, Osaka 589-8511, Japan. Phone and fax: 81-72-367-7600. E-mail: masaaki@med.kindai.ac.jp.

▽ Published ahead of print on 10 September 2008.

prototypic ecotropic gammaretrovirus, and defective spleen focus-forming virus (SFFV). When integrated into erythroid progenitor cells, the SFFV component induces rapid proliferation and differentiation of these target cells, causing increased hematocrit values (polycythemia) and massive splenomegaly within a few weeks after inoculation into a susceptible strain of mice (5, 32, 36). This increase in the number of erythroid progenitor cells leads to increasing copy numbers of F-MuLV and SFFV proviruses and ultimately causes the emergence of erythroleukemia through promoter insertion or silencing of a tumor suppressor gene (22). The pathogenicity of FV is, however, influenced by several host genes: some directly restrict the target cell entry or integration of F-MuLV and SFFV, and others interfere with the growth potentiation of SFFV-infected erythroid progenitor cells (5, 32, 36). Yet other host genes, however, influence the FV-induced pathogenesis more indirectly by affecting the host immune response to the viral antigens. These include the major histocompatibility complex class I and class II genes that regulate $CD8^+$ and $CD4^+$ T-cell recognition of viral epitopes (33, 34); a class Ib gene putatively influencing natural killer cell activities toward FV-infected cells (18, 35); and a non-major histocompatibility complex gene, *Rfv3*, that influences the duration of viremia (6, 17, 47) partly through its effects on the production of virus-neutralizing antibodies (Ab) (23). The *Rfv3* gene has been mapped to within a narrow segment of mouse chromosome 15, colocalizing with the *APOBEC3* locus (23, 36), indicating that the possible polymorphisms in the *APOBEC3* locus might constitute a physiological resistance factor to FV infection in mice. We demonstrate here that an allelic variant of mAPOBEC3 expressed in C57BL/6 mice does restrict F-MuLV replication as well as FV-induced pathogenesis in vivo.

MATERIALS AND METHODS

Mice and virus. C57BL/6, BALB/c, B10.A/SgSn, and (BALB/c × C57BL/6)F_1 ($CB6F_1$) mice were purchased from Japan SLC, Inc., Hamamatsu, Japan. A/WySnJ mice were purchased from the Jackson Laboratory, Bar Harbor, ME. The mAPOBEC3-deficient mice have been described previously (31). They were backcrossed to C57BL/6 mice at least seven times and mated with BALB/c mice. Both male and female mice, 6 to 10 weeks old, were used for virus inoculation. All animals were housed and bred in the experimental animal facilities at Kinki University School of Medicine under a specific-pathogen-free condition, and the experiments described here have been approved by Kinki University. Replication-competent helper virus of the FV complex, F-MuLV, was purified from the culture supernatant of *Mus dunni* cells persistently infected with an infectious molecular clone, FB29 (44), as described previously (33).

Vector constructions. Total RNA was extracted from tissues and cells by using TRIzol reagent (Invitrogen, Carlsbad, CA), and cDNA synthesis was performed by using a SuperScriptIII first-strand synthesis system (Invitrogen). The primers described below were purchased from GeneDesign, Inc., Osaka, or Operon Biotechnologies, Tokyo, Japan. The full-length mAPOBEC3 cDNA were amplified by PCR using the oligonucleotide primers 5′-GGGGTACCGCCGCCACC ATGGGACCATTCTGTCTGGGATGCAGCCATCGC-3′ and 5′-GGTCTAG ACATCGGGGGTCCAAGCTGTAGGTTTCC-3′, with primary cDNA samples prepared from the spleens of C57BL/6 and BALB/c mice. The hAPOBEC3G and hAPOBEC3F cDNA were amplified by PCR using the primers 5′-GGGGTACCG CCGCCACCATGAAGCCTCACTTCAGAAACACAGTGGAGCG-3′ (for both hAPOBEC3G and hAPOBEC3F) and 5′-GGACCGGTGTTTTCCTGATTCTGG AGAATGGCCCGC-3′ (for hAPOBEC3G) or 5′-GGACCGGTCTCGAGAATC TCCTGCAGCTTGCTGTCCAGG-3′ (for hAPOBEC3F), with templates prepared from peripheral blood mononuclear cells of a healthy individual. The above-described APOBEC3 cDNA were cloned into the SalI/EcoRI digest (for mAPOBEC3) or HindIII/KpnI digest (for hAPOBEC3) of the pFLAG-CMV2 vector (Sigma-Aldrich Corp., St. Louis, MO.). The control plasmid pFLAG-CMV2-GFP was constructed by amplifying the green fluorescent protein (GFP) gene from the pEGFP vector (Clontech Laboratories, Inc., Mountain View, CA) with the oligonucleotide primers 5′-GGAAGCTTATGGTGAGCAAGGGCGAGGAGC-3′ and 5′-TCAGTACTTGTACAGCTCGTCCATGCCG-3′ and inserting it into the HindIII/EcoRI digest of the pFLAG-CMV2 vector.

The catalytic site mutants were produced based on the mAPOBEC3 cDNA lacking the exon 5 cloned from C57BL/6 mice ($mA3^b\Delta5$) by a quick-change site-directed mutagenesis using the pFLAG-CMV2-$mA3^b\Delta5$ plasmid as the template. The following primers were used to introduce each mutation (underlined). Primers 5′-CAACATCCACGCTGCAATCTGCTTTTTATACTGGTTCCATG ACAAAGTACTGAAAGTGCTGTCTCCG-3′ and 5′-GTACTTTGTCATGG AACCAGTATAAAAAGCAGATTGCAGCGTGGATGTTGTCCTTGTTCT TAAAGACCCC-3′ were used for the generation of $mA3^b\Delta5^{E73A}$, and primers 5′-AAAGGCAAACAGCATGCAGCAATCCTCTTCCTTGATAAG-3′ and 5′-TCTTATCAAGGAAGAGGATTGCTGCATGCTGTTTGCC-3′ were used for the generation of $mA3^b\Delta5^{E257A}$. The double mutant $mA3^b\Delta5^{E73A\ E257A}$ was generated on pFLAG-CMV2-$mA3^b\Delta5^{E257A}$ by using the oligonucleotide pairs used for the generation of $mA3^b\Delta5^{E73A}$. These mutants were verified by DNA sequencing. The plasmids expressing the chimera between $mA3^b\Delta5$ and the mAPOBEC3 lacking the exon 5 cloned from BALB/c mice ($mA3^d\Delta5$), pFLAG-CMV2-$mA3^d\Delta5$/$mA3^b\Delta5$ and the reciprocal, pFLAG-CMV2-$mA3^b\Delta5$/$mA3^d\Delta5$, were constructed by mutually exchanging the cytidine deaminase catalytic domain 2 (CDD2)-encoding fragments between the $mA3^b\Delta5$ and the $mA3^d\Delta5$ cDNA at the unique HindIII site.

The plasmid vectors used for the establishment of stably expressing cells, the pIRES-PURO-FLAG-mA3, pIRES-PURO-FLAG-hA3, pIRES-PURO-FLAG, and pIRES-PURO-FLAG-GFP plasmids, were constructed by inserting the SpeI-XbaI fragment from the pFLAG-CMV2-mA3, pFLAG-CMV2-hA3, pFLAG-CMV2, and pFLAG-CMV2-GFP plasmids, respectively, into the SpeI/NheI digest of the pIRES-PURO vector (Clontech Laboratories, Inc.). These constructs were verified by DNA sequencing.

Establishment of stably transfected cell lines. To determine the possible restricting effects of the mAPOBEC3 allelic variants in a focus formation assay that mimics physiological MuLV replication, we established BALB/3T3 cell lines that stably expressed different FLAG-tagged versions of mAPOBEC3, the short isoform of mAPOBEC3 derived from C57BL/6 mice ($mA3^b\Delta5$) and the full-length ($mA3^d$) and the short ($mA3^d\Delta5$) isoforms derived from BALB/c mice (Fig. 1). DNA transfection into BALB/3T3 cells was performed by using Lipofectamine 2000 reagent (Invitrogen). For the establishment of stable transfectants, cells expressing FLAG peptide (FLAG) and FLAG-fusion proteins (FLAG-proteins) were selected in the presence of 6 μg/ml puromycin (Sigma-Aldrich) and 200 μg/ml Geneticin (GIBCO Industries Inc., Los Angeles, CA), and colony-forming cells were picked into a well of 96-well culture plates. The expression of FLAG and FLAG-proteins was confirmed by immunoblotting analyses of the cell lysates and with immunofluorescence staining of the cells.

PCR analysis of mAPOBEC3 mRNA and genomic DNA. Endogenous mAPO BEC3 and GAPDH mRNA from tissues and cells were detected by reverse transcription-PCR (RT-PCR) using primers 5′-GGGGTACCGCCGCCAC CATGGGACCATTCTGTCTGGGATGCAGCCATCGC-3′ and 5′-GGTCTA GACATCGGGGGTCCAAGCTGTAGGTTTCC-3′ for the full-length mAPO BEC3; primers 5′-TTACAAATTTTAGATACCAGGATTCTAAGCTTCAGG AG-3′ and 5′-TTGGTTGTAAAACTGCGAGTAAAATTCCTCTTCAC-3′ for the mAPOBEC3 exon 5 region; and primers 5′-GCCAAGGCTATCCATGAC AACTTTGG-3′ and 5′-GCCTGCTTCACCACCTTCTTGATGTC-3′ for mouse GAPDH. Genomic allele analyses of APOBEC3-deficient mice were done by detecting the insertion of a neomycin resistance gene in the exon 3 (31) by using the oligonucleotide primers 5′-CCCCCCAAGGACAACATCCACGCTG-3′ and 5′-GGCGGCAGGCGATTCAGGCCTTGGAA-3′.

Quantitative real-time PCR analyses of mAPOBEC3 mRNA. Real-time PCR assays for quantitative comparisons of mAPOBEC3 mRNA expression levels were performed as described previously (36). The mAPOBEC3 fragment was amplified from 50 ng of total cDNA and quantified using Platinum Quantitative PCR SuperMix-UDG with 6-carboxyl-X-rhodamine (ROX) reference dye (Invitrogen) with an Applied Biosystems 7900HT Fast Real-Time PCR system (Applied Biosystems, Foster City, CA). The primers and 6-carboxyfluorescein (FAM) dye-labeled probe used for the quantification of mAPOBEC3 messages were as follows. Primers were 5′-GCGGCTCCACAGGATCAA-3′ and 5′-TCC AAGCTGTAGGTTTCCAAAGT-3′; and the probe was 5′-TCTGCAAGATT GGTGAAT-3′. After initial incubations at 50°C for 2 min and 95°C for 10 min, 40 cycles of amplification were carried out for 15 s at 95°C, followed by 1 min at 60°C. TaqMan rodent GAPDH control reagent (Applied Biosystems) was used as an internal control.

Northern and Western blot analyses. Total RNA was prepared from mouse tissues by using TRIzol reagent. Two micrograms of the RNA was denatured

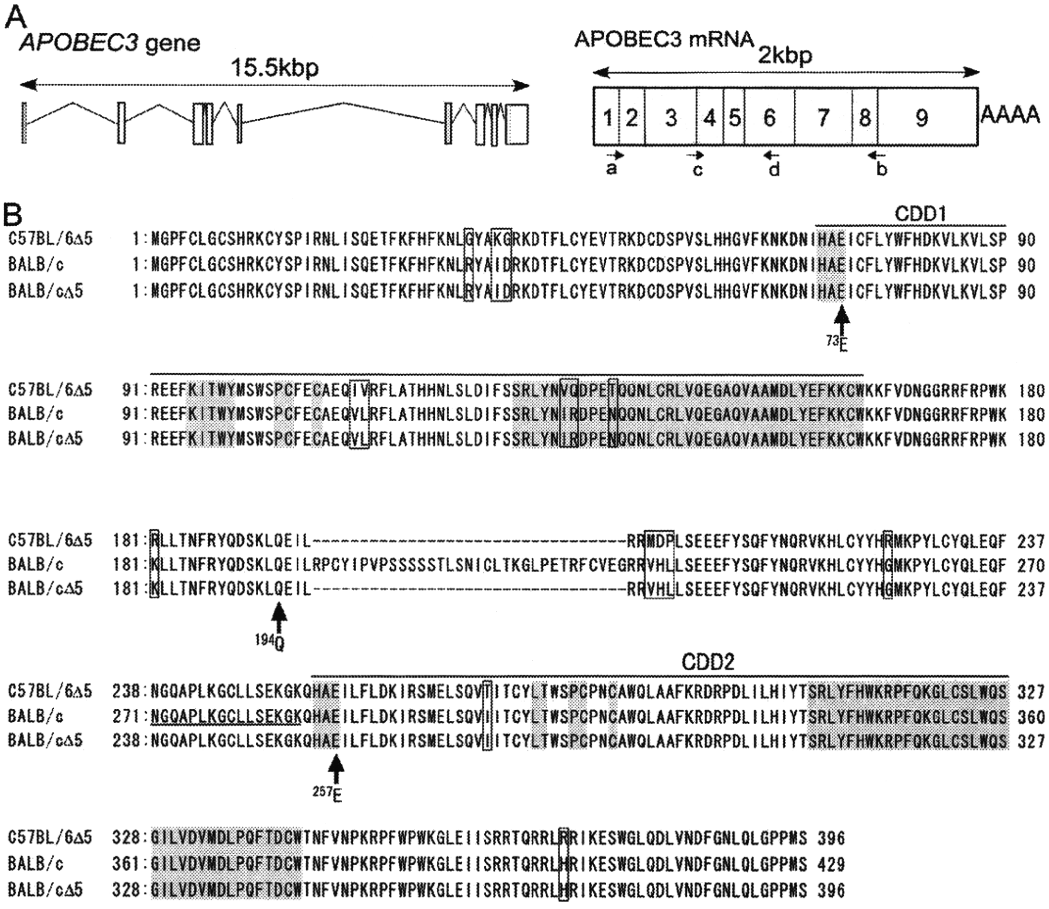

FIG. 1. Alleles and isoforms of mAPOBEC3 in FV-resistant C57BL/6 and -susceptible BALB/c mice. (A) The known genomic organization and splicing pattern of the mouse *APOBEC3* gene is shown with short arrows indicating the positions of the PCR primers used. (B) Alignment of the amino acid sequences of mAPOBEC3 for the C57BL/6-derived exon 5-lacking isoform ($mA3^{b}\Delta5$) (GenBank accession no. NM_030255), and BALB/c-derived full-length ($mA3^{d}$) [BC003314] and exon 5-lacking ($mA3^{d}\Delta5$) isoforms (GenBank accession no. EDL04624). Open boxes show different amino acid residues, shaded boxes show the regions necessary for CDD activities, and the long horizontal lines indicate two CDDs as described in previous reports (15, 37). B10.A/SgSn mice showed amAPOBEC3 sequence that was completely identical to that of C57BL/6 mice, while A/WySn mice shared the mAPOBEC3 sequence with BALB/c mice.

with RNA loading mixture (GenHunter Corporation, Nashville, TN), separated in a 1% formaldehyde-agarose gel, transferred to nitrocellulose membrane, and hybridized with ^{32}P-labeled probes that were prepared by random priming with the templates generated by RT-PCR (mAPOBEC3, 5′-CCCGTCTCCCTTCAC CATGGGG-3′ and 5′-GGGAGACCTTTTGTTAGACAGATATTTGACAGA GTGG-3′; and mouse β-actin, 5′-ATGGATGACGATATCGCTGCGCTGGT CGTCGACAACGGCTCCGGC-3′ and 5′-GGTCATCTTTTCACGGTTGGC CTTAGGGTTCAGGGGGGCC-3′). Specific hybridization was visualized using a BAS-MS imaging plate (Fujifilm Corp., Tokyo, Japan). Densitometric analyses of the detected bands were done by using Image Gauge software (Fujifilm Corp.), and the results were normalized with GAPDH for each sample. Anti-FLAG M2 (Sigma-Aldrich) and anti-actin (Santa Cruz Biotechnology Inc., Santa Cruz, CA) Ab were purchased from the above-mentioned suppliers. Horseradish peroxidase-conjugated secondary Ab was purchased from Zymed Laboratories (San Francisco, CA). Detection by immunoblotting of F-MuLV gp70 and $p30^{gag}$ with monoclonal antibodies (MAb) 720 and R18-7 has been described previously (40).

F-MuLV infection in vitro and APOBEC3 packaging analysis. BALB/3T3 cells stably expressing FLAG-APOBEC3 were seeded at 3×10^4 cells/well in 24-well plates and infected with purified F-MuLV at a multiplicity of infection of 2.0 in the presence of 1 μg/ml Polybrene (Sigma-Aldrich). After 2 h of incubation, the cells were washed, fed with fresh medium, and cultured for 2 days. For packaging analyses, the culture supernatants were centrifuged to remove cells, and viral particles were precipitated with polyethylene glycol and step purified into a 15%/85% sucrose interface (33). For flow cytometry analyses of the surface gp70 expression, F-MuLV-infected transfectants were detached from culture wells with a brief trypsin treatment and stained with biotinylated MAb 720 (40), followed by an incubation with allophycocyanin-conjugated streptavidin (eBioscience Inc., San Diego, CA), and were analyzed with a Becton-Dickinson (Franklin Lakes, NJ) FACScalibur system.

Sequence analysis of proviral DNA. F-MuLV in 1 ml of culture medium were inoculated onto a culture of *Mus dunni* cells and incubated for 18 h. After trypsinization and washing, the cells were treated with RNase I, and their DNA was isolated by using DNeasy (Qiagen, Hilden, Germany). A 1.2-kbp fragment of the F-MuLV proviral genome harboring the U3 and a part of the *gag* sequence was amplified by PCR using the primers 5′-CGGGATCCAAGGACCTGAAA TGACCCTG-3′ and 5′-GAAGAGAGAGGGGAGGTTTAGGG-3′. The amplified fragments were cloned into the pCR-Blunt vector using a Zero Blunt TOPO PCR cloning kit (Invitrogen). Sequencing was performed by using the T7 and T3 primers.

PCR quantification of F-MuLV genomic RNA and integrated proviral DNA. F-MuLV viral RNA in culture medium was purified with a QIAamp viral RNA kit (Qiagen) and cDNA generated by RT with SuperScriptIII First-Strand synthesis system (Invitrogen) after a treatment with DNase I (Invitrogen). Genomic DNA was purified from F-MuLV-infected BALB/3T3 cells expressing FLAG or FLAG-protein or *Mus dunni* cells infected with F-MuLV as described above. Viral DNA was quantified using Platinum Quantitative PCR SuperMix-UDG with ROX and a 7900HT Fast Real-Time PCR system. Primers for the detection of the F-MuLV genome and the FAM-labeled probe were designed for the *env* region by using the following oligonucleotides. Primers were 5′-AAGTCTCCC

CCCGCC-3′ and 5′-AGTGCCTGGTAAGCTCCCTGT-3′; and the FAM-labeled probe was 5′-ACTCCACATTGATTTCCCCGTCC-3′. After initial incubations at 50°C for 2 min and 95°C for 10 min, 40 cycles of amplification were carried out for 30 s at 95°C, followed by 1 min at 60°C. TaqMan rodent GAPDH control reagent was used as an internal control for genomic DNA.

Quantification of F-MuLV gp70 in culture supernatant. Ninety-six-well plates were coated with the gp70-specific MAb 48 (7) at 0.5 mg/well in 0.1 M $NaHCO_3$. Wells were blocked with 10% fetal bovine serum and incubated with a culture supernatant containing F-MuLV for 2 h at room temperature. After washing with PBS containing 0.05% Tween 20, 2 μg/well biotin-conjugated MAb 720 (40) was added and incubated for 1 h. After washing, the plates were incubated with a 1:30,000 dilution of horseradish peroxidase-conjugated streptavidin (Zymed Laboratories), and the chromogenic reaction was performed with 3,3′,5,5′-tetramethylbenzidine (Wako Pure Chemical Industries, Ltd., Osaka, Japan). The assay signals were measured as optical density at 450 nm, and the gp70 concentration was determined by adjusting it to the standard curve set with purified F-MuLV particles.

F-MuLV infection in vivo. C57BL/6 mice were inoculated with 1×10^5 focus-forming units (FFU) of F-MuLV by injecting 0.5 ml of a dilution via the tail vein. The spleen and bone marrow were removed, and single-cell suspensions were prepared for infectious center assays. $CB6F_1$ mice were inoculated with 1×10^4 FFU of F-MuLV.

F-MuLV infectivity and infectious center assays. These assays were performed as described previously (24, 46). In brief, 1 ml of culture supernatant from F-MuLV-infected FLAG- or FLAG-protein-expressing BALB/3T3 cells was diluted serially and plated in duplicate with 1 μg/ml Polybrene on monolayers of *Mus dunni* cells. For infectious center assays, spleen or bone marrow cell suspensions were serially diluted and plated at concentrations between 1.0×10^3 and 1.0×10^6 cells/well onto monolayers of *Mus dunni* cells. After being washed and fixed with methanol on the second day of coculturing, F-MuLV-infected cell foci were visualized with MAb 720 as described previously (40).

FV complex and assessment of its pathogenicity in vivo. A B-tropic FV complex free of lactate dehydrogenase-elevating virus was kindly provided by K. J. Hasenkrug, Laboratory of Persistent Viral Diseases, NIH, NIAID, Rocky Mountain Laboratories, Hamilton, MT. Inoculation of $CB6F_1$ mice with FV complex, monitoring of hematocrit values, and flow cytometry analyses of bone marrow cells were performed as described previously (18, 24).

Statistics. One-way analysis of variance (ANOVA) for the comparison of multiple groups was performed using GraphPad Prism software, version 5.0 (GraphPad Software, Inc., San Diego, CA), with an indicated posttest. When significant differences were pointed out by the ANOVA analyses, an individual level of significance was calculated for each pair of groups by two-tailed Student's or Welch's *t* test, depending on whether the variances were regarded as equal or not, respectively. Frequencies of mutations were evaluated by two-sided Fisher's exact test, between selected groups following an extended Fisher's exact test performed for the entire contingency table.

RESULTS

Allelic differences at the *APOBEC3* locus between FV-resistant and -susceptible strains of mice. The *Rfv3* gene that influences the duration of viremia after FV infection has been mapped to a segment of mouse chromosome 15 harboring the *APOBEC3* gene (17, 23, 36, 47); this led us to explore possible allelic differences in the expression of mAPOBEC3. We found that mAPOBEC3 mRNA expression levels in the hematopoietic tissues from naturally FV-resistant C57BL/6 and B10.A/SgSn mice were higher than those in susceptible BALB/c and A/WySnJ mice (Fig. 2A). Quantitative real-time PCR analyses confirmed that C57BL/6 and B10.A/SgSn mice expressed three- to fourfold higher levels of mAPOBEC3 mRNA than BALB/c and A/WySn mice did, both in the spleen and bone marrow (Fig. 2B). In addition, the mAPOBEC3 isoforms derived from C57BL/6 and BALB/c mice differed at several amino acid residues, five of which were located within the CDD1 (Fig. 1). Interestingly, A/WySnJ mice lacking the ability to control viremia (6) and to produce F-MuLV-neutralizing Ab (23) shared the mAPOBEC3 sequence with BALB/c mice.

Additional variability between mouse strains was also observed in part for the relative amounts of the two splice isoforms of mAPOBEC3. The mAPOBEC3 cDNA obtained by RT-PCR amplification from C57BL/6 mice was slightly smaller than that from BALB/c mice (Fig. 2C), and this was due to the lack of a 99-bp stretch corresponding to the exon 5 (Fig. 1). The use of primers placed in exons 4 and 6 showed that the predominant mAPOBEC3 mRNA isoform expressed in C57BL/6 mice lacked exon 5, while BALB/c mice expressed full-length mAPOBEC3 with very low levels of the short isoform (Fig. 2C). $CB6F_1$ mice expressed readily detectable full-length and truncated isoforms, with the latter in excess. Although the observed differences in the intensities of the PCR product bands might reflect different efficiencies in the amplification of the short and long fragments, the observed high intensity of the short-fragment band in C57BL/6 mice and the low intensity of the long-fragment band in BALB/c mice (Fig. 2C) are in agreement with the results of the Northern blotting (Fig. 2A) and real-time PCR (Fig. 2B) analyses. Thus, it is reasonable to conclude that BALB/c mice express a low level of full-length messages and C57BL/6 mice a high level of truncated mAPOBEC3 messages.

In vitro restriction of F-MuLV replication with C57BL/6-derived mAPOBEC3. It has been shown that mAPOBEC3 lacking the exon 5 (mAPOBEC3Δ5) can be packaged into MuLV particles more efficiently than the full-length mAPOBEC3 protein and, thus, can exert partial restriction of MuLV integration (1), although a recent report (4) has indicated similarly efficient incorporation of the full-length and the exon 5-lacking mAPOBEC3 into MuLV virions. However, the previous reports of the possible restricting effects of mAPOBEC3 on MuLV integration employed acute transfection of mAPOBEC3-expressing vector into MuLV packaging cells and examined a single-round integration of the MuLV vector and resultant expression of an inserted indicator gene. We intended to examine the possible restricting effects of mAPOBEC3 isoforms on more physiological replication cycles of infectious MuLV. Thus, we established BALB/3T3 cell lines that stably expressed different FLAG-tagged versions of mAPOBEC3 and measured the infectivity of F-MuLV produced from the transfectants in a focus formation assay that mimics physiological MuLV replication. BALB/3T3 cells stably expressing hAPOBEC3G, hAPOBEC3F, or GFP were also established as controls. These transfectants expressed comparable levels of APOBEC3 mRNA and produced APOBEC3 proteins of the expected sizes (Fig. 2D and F). Acute infection of the BALB/3T3 lines with an infectious molecular clone of F-MuLV resulted in a similar range of the envelope glycoprotein gp70 detected in the lysates, regardless of the APOBEC proteins expressed (Fig. 2F). The levels of F-MuLV infectivity and gp70 expression in the transfected lines were also confirmed to be similar by flow cytometric analyses (Fig. 2E). However, when we measured the infectivities of progeny viruses produced from the stable transfectants by focus formation assays on fully permissive *Mus dunni* cells, we found wide differences depending on the particular APOBEC3 protein expressed (Fig. 2H). Thus, the infectivity of F-MuLV produced from the $mA3^bΔ5$-expressing cells was drastically reduced to a level similar to that obtained with F-MuLV derived from the hAPOBEC3G-expressing cells, whereas some 2.0×10^4 FFU/ml of infectious particles were

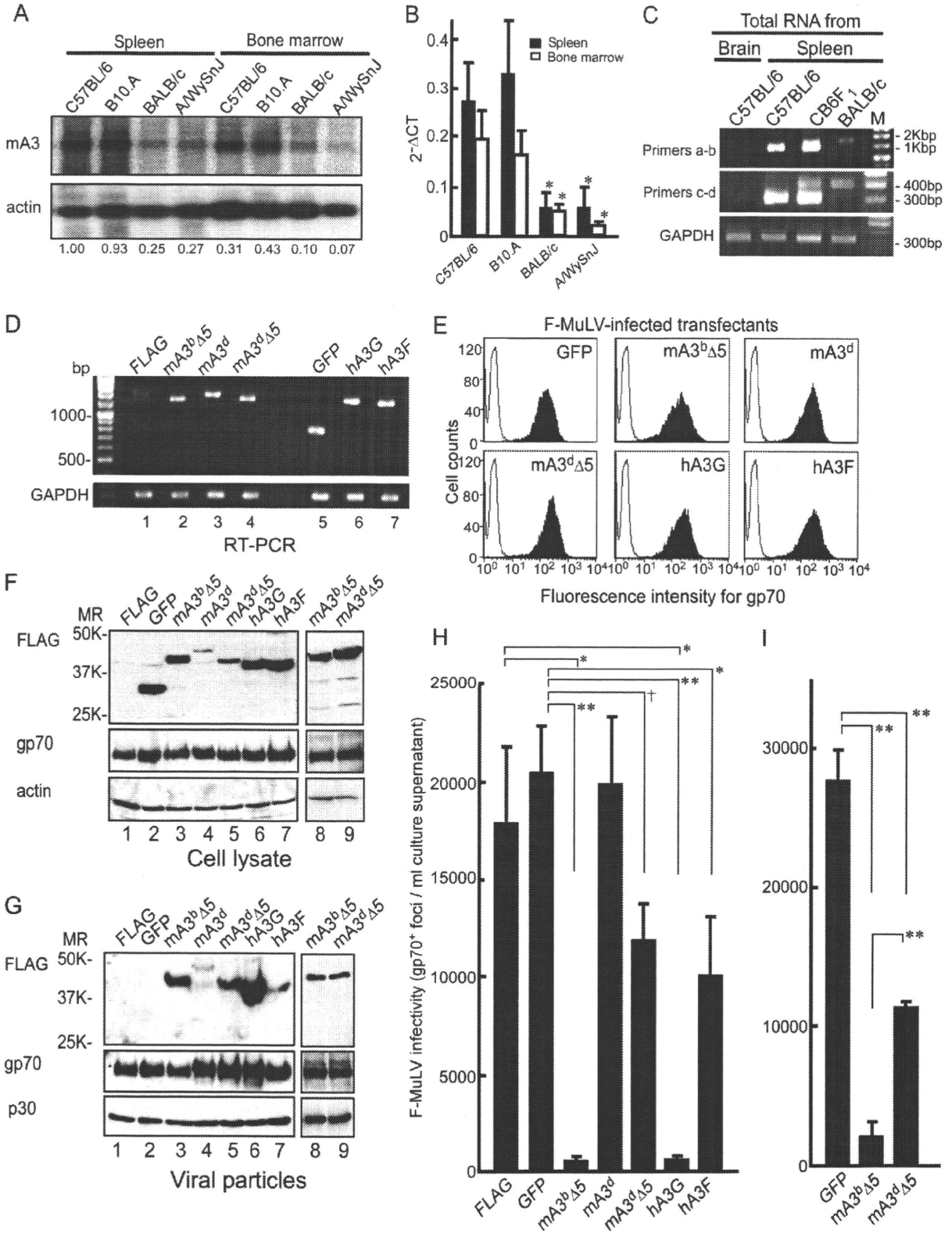

FIG. 2. Expression of the different alleles and isoforms of mAPOBEC3 in FV-resistant and -susceptible mice and infectivities of F-MuLV virions produced from mAPOBEC3-expressing cells. (A) Comparisons of mAPOBEC3 mRNA expression levels between mouse strains, by Northern blotting. Female mice, 7 to 8 weeks old, were analyzed for endogenous mAPOBEC3 mRNA expression. mAPOBEC3 mRNA was detected in 5 μg total RNA extracted from the spleen and bone marrow of the indicated strains of mice. β-Actin was used as an internal control. The numbers shown below each lane indicate densitometric ratios of expression levels between mAPOBEC3 and β-actin messages, normalized to that in the spleen of C57BL/6 mice. (B) Levels of expression of mAPOBEC3 mRNA relative to GAPDH quantified by real-time PCR are shown. Means of three samples each are shown with bars indicating standard errors of the means. *, statistically significant differences from the expression

TABLE 1. Number of F-MuLV provirus, infectious particles, and provirus in cells infected with progeny virus

Stable transfectant	Proviral copy no. (mean ± SEM) in producer cells (10^4)[a]	Concn (μg/ml) of gp70 (mean ± SEM) in culture supernatant[b]	Viral genomic copy no. (mean ± SEM) in culture supernatant (10^6)[c]	Proviral copy no. (mean ± SEM) in indicator cells (10^4)[e]
FLAG	99.47 ± 21.23	87.61 ± 4.76	5.43 ± 0.47	14.38 ± 4.79
GFP	156.80 ± 31.84	70.97 ± 11.17	4.06 ± 0.29	18.89 ± 4.00
mA3^{b}Δ5	140.19 ± 23.25	73.01 ± 7.63	3.17 ± 0.40	0.57 ± 0.05[f]
mA3^d	94.57 ± 24.01	70.71 ± 15.41	5.05 ± 0.71	16.45 ± 1.74
mA3^{d}Δ5	128.18 ± 23.60	72.57 ± 13.27	4.18 ± 0.31	4.59 ± 1.25[f]
hAPOBEC3G	53.78 ± 4.43	53.35 ± 8.44	2.82 ± 0.33[d]	0.35 ± 0.05[f]
hAPOBEC3F	99.80 ± 2.99	65.95 ± 6.05	3.54 ± 0.78	2.55 ± 0.40

[a] F-MuLV proviral DNA was quantified in the genomic DNA of the infected cells by quantitative real-time PCR using an F-MuLV-specific probe and primers. Data shown are means ± standard errors of the means (SEM) of copies per 50 ng of cellular genomic DNA, calculated from three repeated experiments. One-way ANOVA with Tukey's posttest for multiple comparisons indicated a significant difference only between GFP and hAPOBEC3G, but this was not significant ($P = 0.08$) by individual analysis using Welch's t test.

[b] Concentration of F-MuLV structural protein gp70 in culture supernatant from the acutely infected stable transfectants was analyzed by captured enzyme-linked immunosorbent assay using anti-gp70 MAb. Data shown here are means ± SEM calculated from three repeated experiments. No significant differences between the groups were found by one-way ANOVA with Tukey's posttest.

[c] Viral genomic RNA in the culture supernatant from the acutely infected stable transfectants was quantified by quantitative RT-PCR. Data shown here are means ± SEM of copies per 1 ml culture supernatant calculated from 3 repeated experiments. One-way ANOVA with Tukey's posttest indicated a significant group-wise difference only between the FLAG and hA3G.

[d] Student's t test for individual level of significance gave a P value of 0.011.

[e] F-MuLV proviral DNA was quantified from infected *Mus dunni* cells as described in the text. One-way ANOVA with Tukey's posttest for multiple comparisons indicated significant group-wise differences, which were then individually analyzed by t test.

[f] $P < 0.05$, in comparison with that of GFP.

detected when the supernatants from the BALB/3T3 cells expressing FLAG alone or control GFP were tested (Fig. 2H). In contrast, only a marginal reduction in F-MuLV infectivity was observed for the supernatant of mA3^{d}Δ5-expressing cells. Enforcing higher levels of expression of the mA3^d cDNA in the BALB/3T3 cells, compared with a low expression level of the endogenous *mA3^d* allele (Fig. 2D, lanes 1 and 3), did not result in any significant decrease in the infectivity of the virus produced (Fig. 2H), although the detectable amounts of mA3^d protein were apparently lower than those of the exon 5-lacking isoforms in several tested clones, which might have caused inefficient incorporation of the full-length protein into the virions (Fig. 2G). Nevertheless, these results indicate strain-dependent differences in F-MuLV-restricting activities of mAPOBEC3, with the C57BL/6-derived short isoform restricting F-MuLV with an efficacy similar to that shown by heterologous hAPOBEC3G.

When F-MuLV particles were purified from the culture supernatant of acutely infected transfectants, virion-incorporated mAPOBEC3 lacking the exon 5, but not the full-length mAPOBEC3, was readily detectable along with viral gp70 and p30^{gag}, regardless of their strains of origin (Fig. 2G). Interestingly, although mA3^{d}Δ5 derived from BALB/c mice was incorporated into F-MuLV as efficiently as C57BL/6-derived mA3^{b}Δ5 (Fig. 2G), only mA3^{b}Δ5 inhibited F-MuLV replication as strongly as hAPOBEC3G did in vitro (Fig. 2H). To exclude the possibility that the difference observed for the effects of mA3^{b}Δ5 and mA3^{d}Δ5 in restricting F-MuLV replication in vitro was caused by the slightly smaller amount of mA3^{d}Δ5 than mA3^{b}Δ5 detected in the transfectants used (Fig. 2F), we examined separate pairs of the stable transfectants. As shown in lanes 8 and 9 in Fig. 2 F and G, a higher level of mA3^{d}Δ5 was detected in the separate clone of stable transfectant, and the detected levels of virion-incorporated mAPOBEC3Δ5 proteins were similar. Nevertheless, the progeny virus produced from the mA3^{d}Δ5-expressing cells showed only about 60% reduc-

levels in B10.A/SgSn mice, indicated by one-way ANOVA with Dunnett's posttest for multiple comparisons ($P < 0.05$). (C) Splicing variants of the *APOBEC3* gene expressed in C57BL/6 and BALB/c mice. The known genomic organization and splicing pattern of the *APOBEC3* gene along with the positions of the primers used are shown in Fig. 1. The primers a and b amplified the entire mAPOBEC3-coding region, while primers c and d encompassed exons 4 and 6. GAPDH was used as an internal control. (D) Expression of APOBEC3 mRNA in the BALB/3T3 cells stably transfected with each *APOBEC3* gene was analyzed by RT-PCR. The same primers for mAPOBEC3 were used for samples in lanes 1 to 4. Samples in lanes 5 to 8 were amplified with each specific primer set. GAPDH was used as an internal control. Note the faint band of endogenous mA3^d cDNA in lane 1. (E) Flow cytometric analyses of the cell surface expression of F-MuLV gp70 on acutely infected stable transfectants are shown. Cells expressing the indicated genes were infected with F-MuLV at a multiplicity of infection of 2.0 and analyzed for surface gp70 expression with MAb 720 2 days later. (F and G) Proteins detected in cell lysate (F) and virus particles in the culture supernatant (G) from the infected BALB/3T3 cells expressing FLAG and FLAG-proteins are shown. Immunoblot detection was performed with the anti-FLAG, anti-gp70, anti-p30 or anti-actin Ab. (H and I) Infectivities of progeny F-MuLV produced from APOBEC3-expressing BALB/3T3 cells. *Mus dunni* cells were infected with the progeny virus produced from the indicated transfectants, and foci of infected cells were stained with anti-gp70 MAb for enumeration. The vertical axis in panel I shows F-MuLV infectivity as in panel H. The infectivities are shown as an equivalent of infectious virus per 1 ml of culture supernatant ($n = 3$, mean ± standard deviation; *, $P < 0.05$; †, $P < 0.01$; **, $P < 0.005$). The F-MuLV infectivity detected in the supernatant of hAPOBEC3G-expressing cells was drastically reduced, while only a moderate reduction in F-MuLV infectivity was observed when the indicator cells were inoculated with the supernatant from the hAPOBEC3F-expressing cells, consistent with the previous reports (1, 4, 13). All the experiments shown in panels C to I were performed with at least two representative clones of stable transfectants for each gene, and the results obtained with the independent clones were in agreement with the data shown.

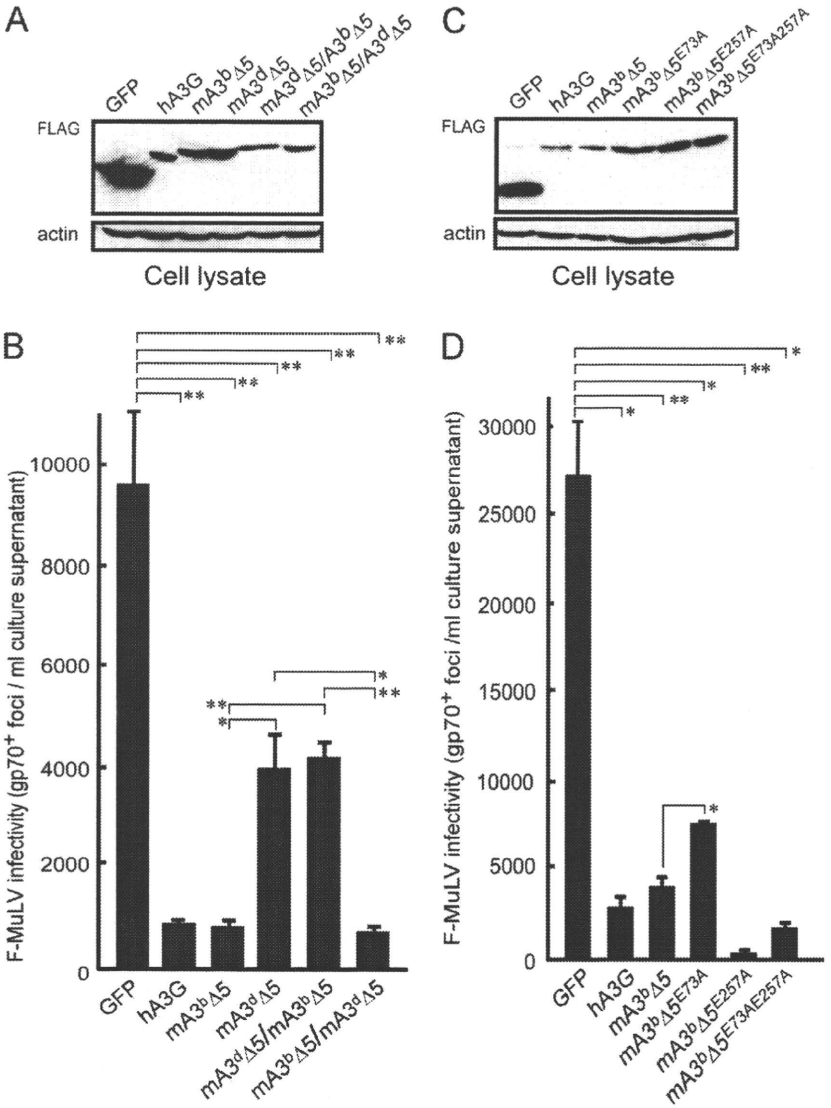

FIG. 3. Infectivities of F-MuLV virions produced from BALB/3T3 cells expressing mA3^{b}Δ5 mutants. (A and C) Cell lysates from the acutely infected transfectants were analyzed for the presence of APOBEC3 proteins. Immunoblot detection was performed with anti-FLAG and anti-actin Ab. (B and D) *Mus dunni* cells were infected with virus produced from the mAPOBEC3Δ5-expressing BALB/3T3 cells, and foci of gp70$^+$-infected cells were enumerated (n = 3, mean ± standard deviation; *, $P < 0.05$; **, $P < 0.005$). All the experiments shown were performed with at least two representative clones of stable transfectants for each gene, and the results obtained with the independent clones were in agreement with the data shown here.

tion in F-MuLV infectivity, while the progeny virus produced from the mA3^{b}Δ5-expressing cells showed vastly reduced infectivity, which was significantly lower than that shown by the mA3^{d}Δ5-containing F-MuLV.

The effectiveness of virion-incorporated mAPOBEC3 in restricting F-MuLV replication was further confirmed by quantitative analyses of viral copy numbers. Whereas neither the numbers of F-MuLV proviruses within the acutely infected stable transfectants nor the amounts of viral gp70 and genomic RNA in the supernatants were significantly different, regardless of the APOBEC3 or control genes expressed by the transfectants (Table 1), with the exception of a slight reduction in viral RNA in supernatants from the hAPOBEC3G-expressing cells, the number of F-MuLV proviral copies detected in infected *Mus dunni* indicator cells was reduced to less than 1/20 of the number detected in the cells infected with the control preparations when progeny virions were produced from mA3^{b}Δ5- or hAPOBEC3G-expressing cells. The number of proviral copies in the indicator cells was only moderately reduced when infected with progeny viruses produced from the mA3^{d}Δ5-expressing cells, and no reduction in the proviral copy numbers was observed for the cells infected with the virus produced from cells expressing the full-length mA3^d (Table 1). Thus, in agreement with the results of the infectious focus formation assays (Fig. 2H and I), mA3^{b}Δ5 restricts F-MuLV proviral integration more efficiently than does mA3^{d}Δ5.

C57BL/6-derived mAPOBEC3 restricts F-MuLV replication in the absence of the deaminase catalytic site. The above-

TABLE 2. Sequence variations of F-MuLV proviral genome observed for infected cells

Stable transfectant	Total no. of nucleotides analyzed[a]	No. of nucleotide exchanges[b]		
		G/A	C/T	Other mutations
FLAG	94,429	0	3	6
GFP	101,856	0	2	6
mA3^{b}Δ5	96,551	3	2	9
mA3^d	94,429	5[c]	0	5
mA3^{d}Δ5	90,185	3	2	5
hAPOBEC3G	95,490	55[d]	5	11
hAPOBEC3F	97,612	2	0	6

[a] A 1,061-nucleotide fragment between the U3 and *gag* sequences from the F-MuLV proviral DNA was cloned, and its sequence was analyzed for at least 90 clones.

[b] The entire contingency table was analyzed for the possible presence of group-wise difference, which indicated a P value of <0.001. An individual group-wise difference was then analyzed by Fisher's exact test.

[c] $P = 0.026$ in comparison with that of GFP but was not significant in comparison with that of FLAG.

[d] $P = 5.77 \times 10^{-17}$ in comparison with the data for FLAG, 4.55×10^{-18}, in comparison with that of GFP.

described results indicate that the major difference between the efficacies of the C57BL/6- and BALB/c-derived mAPOBEC3 proteins in restricting F-MuLV infection in vitro likely stems from the differences in their amino acid sequences (Fig. 1). To analyze this, we constructed reciprocal chimeras between mA3^{b}Δ5 and mA3^{d}Δ5 by mutually exchanging the N-terminal portion at ^{194}Q (Fig. 1) and established BALB/3T3 lines stably expressing the chimeric mAPOBEC3 (Fig. 3A). The progeny virus produced from the cells expressing the chimeric mA3^{d}Δ5/mA3^{b}Δ5 protein, with its N-terminal portion encoded by the BALB/c-derived *mA3^d*, failed to fully restrict F-MuLV replication, while the reciprocal mA3^{b}Δ5/mA3^{d}Δ5 construct restricted F-MuLV replication as efficiently as mA3^{b}Δ5 did (Fig. 3B). These results clearly localized the strain-dependent functional difference of mAPOBEC3Δ5 to the N-terminal portion harboring the CDD1.

It is not clear to what extent APOBEC3 proteins restrict retroviral integration through their deaminase activity as opposed to through a deaminase-independent mechanism (1, 4, 38, 39, 43). Sequencing of the multiple proviral genomes revealed a significant increase in G-to-A mutations in the *Mus dunni* cells infected with F-MuLV produced from the hAPOBEC3G-expressing cells (Table 2). Surprisingly, the proviruses cloned from the indicator cells infected with F-MuLV produced from the mA3^{b}Δ5-expressing cells did not show such a significant increase in G-to-A mutations in comparison with those observed for the cells infected with the control viruses. To further determine if the deaminase activity is required for the observed restriction of F-MuLV replication by mA3^{b}Δ5, mutations were introduced into its catalytic sites. mAPOBEC3, as well as hAPOBEC3G and hAPOBEC3F, harbors two CDD, of which only CDD2 is catalytically active in hAPOBEC3G (37, 38), while CDD1 is active in mAPOBEC3 (15). Mutation of the glutamic acid to alanine at position 73 (E73A) within CDD1, but not the equivalent mutation (E257A) within CDD2, abrogates mAPOBEC3 deaminase activity, as well as antiviral restriction, against *vif*-deficient HIV (15). We introduced these point mutations either individually or in combination into mA3^{b}Δ5 and generated stable transfectants in BALB/3T3 cells (Fig. 3C). The F-MuLV progeny viruses produced from all the mutant mA3^{b}Δ5 transfectants had reduced replicative activities in *Mus dunni* cells (Fig. 3D) in comparison with the virus produced from the control cells, regardless of the introduced mutation(s) into mAPOBEC3, although the E73A mutant showed a slightly reduced repressive activity, implicating some role for this catalytic site. These results, along with the lack of an evident increase in G-to-A substitutions in the integrated proviral genome (Table 2), indicate that mA3^{b}Δ5 may restrict F-MuLV replication in a deaminase-independent fashion.

C57BL/6-derived mAPOBEC3 restricts F-MuLV replication in vivo. The reduced infectivity of the progeny F-MuLV produced from the stably transfected cell lines might have resulted from an excessive amount of mAPOBEC3 protein that was forcibly incorporated into the virion. To examine directly the possible physiological effect of the putative resistant allele, *mA3^b*, on F-MuLV infection in vivo, we introduced the targeted disruption of the *APOBEC3* gene (31) into C57BL/6 mice by backcrossing. The progenies of heterozygous breeding pairs were genotyped (Fig. 4A), and the expression or lack of expression of the *mA3^b* allele in the spleen and bone marrow was confirmed by RT-PCR (Fig. 4B). Infectious center assays revealed that C57BL/6 mice deficient in mAPOBEC3 possessed nearly 100-fold higher numbers of F-MuLV-producing cells at postinfection day (PID) 6, both in the spleen and bone marrow, in comparison with that of the wild-type or heterozygous counterparts (Fig. 4C). To further determine if the allelic difference in the *APOBEC3* locus influences resistance to F-MuLV infection, heterozygous C57BL/6 *mA3$^{b/-}$* mice were mated with BALB/c mice, and the resultant CB6F$_1$ mice were genotyped and infected with F-MuLV. As expected, CB6F$_1$ mice of the *mA3$^{d/-}$* genotype expressed low levels of the full-length, as well as the short mAPOBEC3, mRNA in the bone marrow, while the *mA3$^{d/b}$* mice expressed a higher level of the mA3^{b}Δ5 message along with a low level of the full-length mA3^d mRNA (Fig. 4D). Importantly, *mA3$^{d/-}$* mice deficient in the C57BL/6-derived APOBEC3 protein harbored more than 100-times-larger numbers of F-MuLV-producing cells in their bone marrow than the wild-type *mA3$^{d/b}$* mice at PID 6, despite the expression of the BALB/c-derived *mA3^d* allele (Fig. 4E). Thus, the C57BL/6-derived *mA3^b* allele dominantly confers resistance to F-MuLV infection in the presence of the *mA3^d* allele.

C57BL/6-derived mAPOBEC3 restricts erythroid cell proliferation in mice infected with the pathogenic FV complex. To further determine if the *mA3^b* allele physiologically functions in conferring resistance to FV-induced pathogenesis, FV-susceptible CB6F$_1$ mice possessing or lacking the *mA3^b* allele were infected with FV. CB6F$_1$ *mA3$^{d/b}$* mice possessed on average 13.1% ± 9.2% gp70-positive (gp70$^+$) cells in their bone marrow at PID 7 (Fig. 4F), a large majority of which belonged to the TER119$^+$ erythroblast population (25). On the other hand, when CB6F$_1$ mice lacking the *mA3^b* allele were infected with FV, significantly increased numbers (35.6% ± 11.9%, $P = 0.00015$) of bone marrow cells became positive for gp70, and these included more immature TER-119 cells. Reflecting the above differences, CB6F$_1$ *mA3$^{d/-}$* mice uniformly possessed extremely high hematocrit values at PID 21, while hematocrit

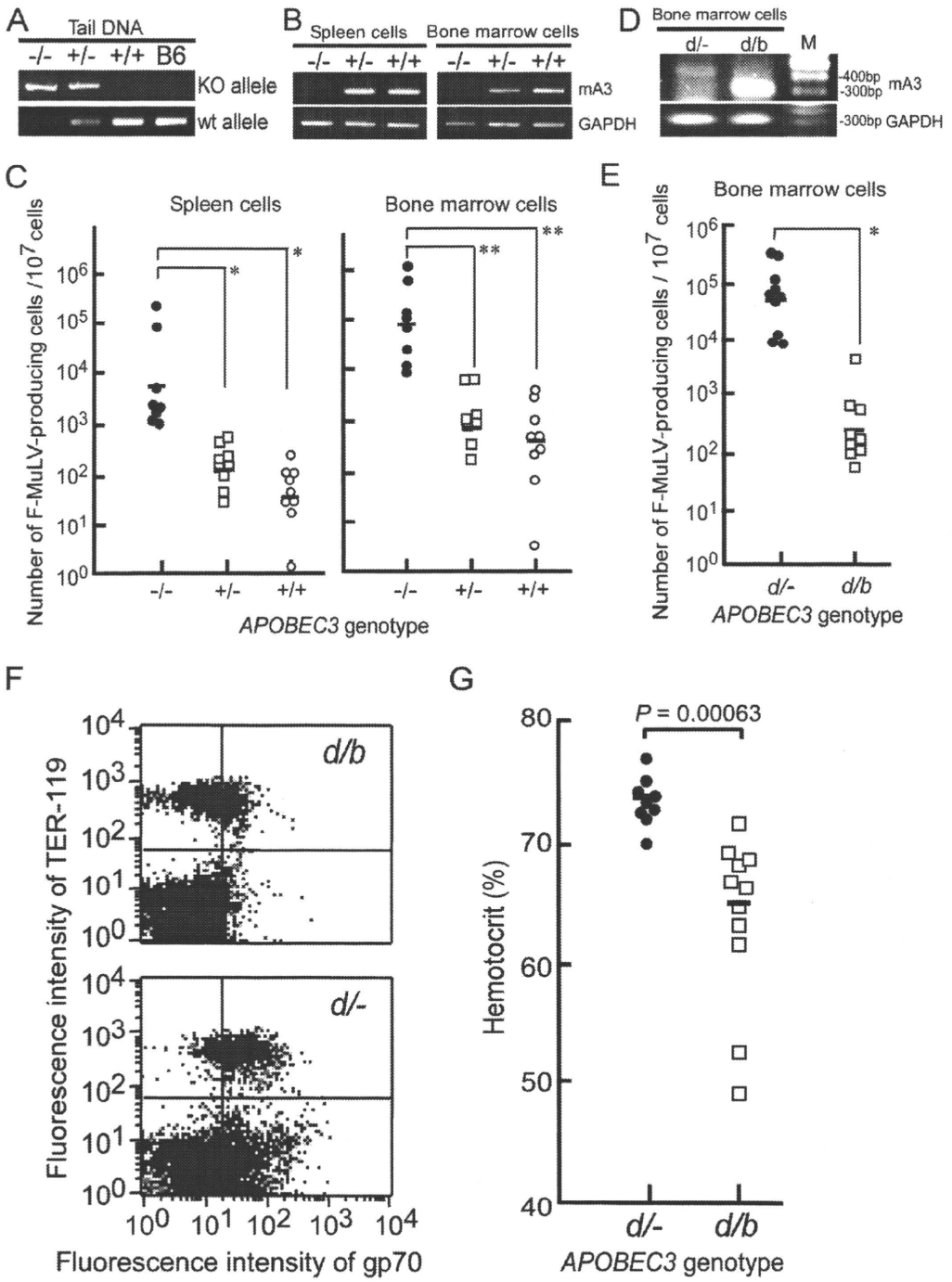

FIG. 4. Replication of F-MuLV in mAPOBEC3-deficient mice and the development of FV-induced disease in vivo. (A) Representative results for genotyping of the *APOBEC3* alleles by PCR. (B) Expression of mAPOBEC3 mRNA in the bone marrow and spleen of the APOBEC3-deficient C57BL/6 mice analyzed by RT-PCR is shown. (C) C57BL/6 mice possessing either the $APOBEC3^{-/-}$ (−/−) (n = 8), +/− (n = 10), or +/+ (n = 9) alleles were inoculated intravenously with 10^5 FFU of purified F-MuLV. F-MuLV infectious centers were enumerated on *Mus dunni* cells with anti-gp70 MAb on PID 6. Short horizontal bars indicate the means. *, $P < 0.02$; **, $P < 0.002$. (D) Expression of APOBEC3 mRNA in mAPOBEC3-deficient $CB6F_1$ mice analyzed by RT-PCR. (E) $CB6F_1$ mice possessing either the $APOBEC3^{d/-}$ (d/−) (n = 10) or d/b (n = 10) alleles were inoculated intravenously with 10^4 FFU of purified F-MuLV. F-MuLV infectious centers in the bone marrow were enumerated by coculturing *Mus dunni* cells and staining with anti-gp70 MAb on PID 6. Short horizontal bars indicate the means. The difference between the groups was analyzed by Student's t test: *, $P < 1 \times 10^{-7}$. (F and G) $CB6F_1$ mice possessing either the $APOBEC3^{d/-}$ (d/−) or d/b alleles were inoculated intravenously with 150 spleen FFU of FV complex. On PID 7, the cells prepared from the bone marrow were stained for TER119 and gp70 and were analyzed by flow cytometry (F). Five mice of each genotype were examined to calculate the means described in the text, and the dot graphs shown are of representative animals. On PID 21, hematocrit values were determined in the peripheral blood (G).

values for the *mA3*$^{d/b}$ mice were significantly lower (Fig. 4G). Thus, the *mA3*^{b} allele does confer resistance to FV-induced erythroid pathology.

DISCUSSION

It has been generally accepted that retroviruses have evolved to evade the antiviral activities of their natural host's APOBEC proteins. In fact, primate lentiviruses counter the action of primate A3G with their Vif protein, while Vif is unable to counteract mAPOBEC3 and HIV-1 is highly susceptible to restriction by mAPOBEC3 (28, 42). The primate APOBEC3G gene predates HIV-related lentiviruses and has been under strong selective pressure for its conserved functionality (41). Thus, physiological targets of primate APOBEC3G might be endogenous retroviruses and nonautonomous retroelements (10, 14). Similarly, MuLV has also evolved mechanisms to block mAPOBEC3. These include the competitive exclusion of mAPOBEC3 from MuLV particles (1, 13), cleavage of virion-incorporated mAPOBEC3 by viral protease (1), and inhibition of the deaminase activity (4). However, possible inhibitory roles of APOBEC3 proteins on exogenous retroviral infection in vivo have become evident through the study of human lentiviruses. Thus, the patterns of hypermutation of HIV from infected individuals have indicated that the hAPOBEC3 proteins fulfill an inhibitory role (2, 26), and the levels of hAPOBE C3G expression have been associated with suppression of HIV-1 viremia and HIV-1-exposed but -uninfected status (3, 20). Regarding the mouse, however, the only previously demonstrated target for mAPOBEC3 in vivo was the betaretrovirus MMTV, with mAPOBEC3-deficient mice giving increased viral replication (39). Although putatively residual activities exerted by mAPOBEC3Δ5 in inhibiting MuLV integration have been reported (1, 4), these might have been caused by an excessive amount of mAPOBEC3 protein forcibly incorporated into the virion, especially when the experiments were performed by transfecting MuLV packaging cells with an mAPOBEC3-expressing plasmid vector.

Based on our previous demonstration that the FV resistance gene *Rfv3* colocalized with the *APOBEC3* locus (23, 36), we have shown here that the mouse gammaretrovirus F-MuLV is a target for mAPOBEC3 and, further, that mAPOBEC3 acts to restrict viral pathogenesis in vivo (Fig. 4). Gammaretroviruses have coevolved with their natural hosts (48), with MuLV and related endogenous retroviruses distributed more widely than MMTV among murine strains and species. Nevertheless, C57BL/6 and closely related C57BL/10 (B10) mice possess multiple host factors that make these strains resistant to FV-induced disease development (5, 22, 32, 36). We have shown in the present paper that differences in the sequence of mAPO BEC3 (Fig. 1), along with different expression levels in the hematopoietic tissues (Fig. 2A to C) account for part of this polymorphism. Further, we have also localized the functional difference between F-MuLV-restricting mA3^{b}Δ5 and less-restricting mA3^{d}Δ5 to the N-terminal portion other than the deaminase catalytic site (Fig. 3). Thus, F-MuLV infection in mice may not only provide a tractable model for the study of the in vivo mechanism of APOBEC3-mediated retroviral restriction, it may also provide insight into mechanisms of virus-host coevolution.

Finally, whether or not the *Rfv3* locus is identical to the *APOBEC3* locus must be discussed. The *Rfv3* gene was first described by comparing the persistence of viremia after FV infection between the prototypic FV-resistant B10.A/SgSn and the susceptible A/WySn mice that share the same *H-2*^{a} haplotype (6). A/WySn mice remained viremic at more than 30 days after FV infection, while B10.A/SgSn mice had cleared viremia by PID 30. Since F_1 crosses between these two strains were not viremic and about half of the (B10.A × A/WySn) × A/WySn backcross mice showed viremia at PID 30, the presence of a recessive host gene in A/WySn mice was postulated in association with the persistence of viremia and was designated the *Rfv3*^{s} allele. Thus, B10.A/SgSn mice possess a dominant allele, the *Rfv3*^{r}, conferring the early clearance of viremia. The *Rfv3* locus was later mapped to within chromosome 15 (17, 47). As we have shown here (Fig. 1), B10.A/SgSn mice share the *APOBEC3* sequence with C57BL/6 and A/WySn with BALB/c. Therefore, it is conceivable that the FV-restricting *mA3*^{b} allele in B10.A/SgSn mice functioned to limit the replication of FV and thus contributed to the observed earlier clearance of viremia. However, for the clearance of viremia in FV-infected mice, the host immune responses are also required. In fact, B-cell-deficient C57BL/6 mice possessed higher levels of viremia than their wild-type counterparts at PID 7 (30), and FV-producing cells in the bone marrow and spleen could not be eliminated, even after effective priming of T cells with the viral antigens, in the absence of Ab-producing cells (24, 30). Thus, although the *mA3*^{b} allele does contribute to the reduction in the number of virus-producing cells in the early stage of FV infection (Fig. 4), it must influence the immune responses, either directly or indirectly, to explain the phenotypes influenced by the *Rfv3* gene. In this regard, (B10.A × A/WySn)F_1 mice do produce F-MuLV-neutralizing Ab earlier than A/WySn mice do (23). The less massive expansion of FV-infected erythroid cells in the *mA3*^{b}-possessing mice than in those lacking this resistant genotype (Fig. 4) might result in the possible preservation of the stromal architecture that is required for cell-to-cell interactions involved in lymphocyte priming and B-cell activation. Further studies are required to clarify the presumable identity of the mouse *APOBEC3* gene as the *Rfv3* gene.

ACKNOWLEDGMENTS

This work was supported in part by grants-in-aid for scientific research from the Ministry of Education, Culture, Sports, Science and Technology of Japan, including the High-Tech Research Center project, and grants from the Ministry of Health, Labor and Welfare of Japan, the Japan Health Sciences Foundation, and the Naito Foundation.

We thank J. B. Dowell for critical readings and corrections of the manuscript.

REFERENCES

1. **Abudu, A., A. Takaori-Kondo, T. Izumi, K. Shirakawa, M. Kobayashi, A. Sasada, K. Fukunaga, and T. Uchiyama.** 2006. Murine retrovirus escapes from murine APOBEC3 via two distinct novel mechanisms. Curr. Biol. **16:**1565–1570.
2. **Beale, R. C., S. K. Petersen-Mahrt, I. N. Watt, R. S. Harris, C. Rada, and M. S. Neuberger.** 2004. Comparison of the differential context-dependence of DNA deamination by APOBEC enzymes: correlation with mutation spectra *in vivo*. J. Mol. Biol. **337:**585–596.
3. **Biasin, M., L. Piacentini, S. Lo Caputo, Y. Kanari, G. Magri, D. Trabattoni, V. Naddeo, L. Lopalco, A. Clivio, E. Cesana, F. Fasano, C. Bergamaschi, F. Mazzotta, M. Miyazawa, and M. Clerici.** 2007. Apolipoprotein B mRNA-

editing enzyme, catalytic polypeptide-like 3G: a possible role in the resistance to HIV of HIV-exposed seronegative individuals. J. Infect. Dis. **195:** 960–964.
4. **Browne, E. P., and D. R. Littman.** 2008. Species-specific restriction of Apobec3-mediated hypermutation. J. Virol. **82:**1305–1313.
5. **Chesebro, B., M. Miyazawa, and W. J. Britt.** 1990. Host genetic control of spontaneous and induced immunity to Friend murine retrovirus infection. Annu. Rev. Immunol. **8:**477–499.
6. **Chesebro, B., and K. Wehrly.** 1979. Identification of a non-H-2 gene (Rfv-3) influencing recovery from viremia and leukemia induced by Friend virus complex. Proc. Natl. Acad. Sci. USA **76:**425–429.
7. **Chesebro, B., K. Wehrly, M. Cloyd, W. Britt, J. Portis, J. Collins, and J. Nishio.** 1981. Characterization of mouse monoclonal antibodies specific for Friend murine leukemia virus-induced erythroleukemia cells: Friend-specific and FMR-specific antigens. Virology **112:**131–144.
8. **Chiu, Y. L., and W. C. Greene.** 2006. Multifaceted antiviral actions of APOBEC3 cytidine deaminases. Trends Immunol. **27:**291–297.
9. **Chiu, Y. L., V. B. Soros, J. F. Kreisberg, K. Stopak, W. Yonemoto, and W. C. Greene.** 2005. Cellular APOBEC3G restricts HIV-1 infection in resting $CD4^+$ T cells. Nature **435:**108–114.
10. **Chiu, Y. L., H. E. Witkowska, S. C. Hall, M. Santiago, V. B. Soros, C. Esnault, T. Heidmann, and W. C. Greene.** 2006. High-molecular-mass APOBEC3G complexes restrict Alu retrotransposition. Proc. Natl. Acad. Sci. USA **103:**15588–15593.
11. **Conticello, S. G., R. S. Harris, and M. S. Neuberger.** 2003. The Vif protein of HIV triggers degradation of the human antiretroviral DNA deaminase APOBEC3G. Curr. Biol. **13:**2009–2013.
12. **Delebecque. F., R. Suspene, S. Calattini, N. Casartelli, A. Saib, A. Froment, S. Wain-Hobson, A. Gessain, J. P. Vartanian, and O. Schwartz.** 2006. Restriction of foamy viruses by APOBEC cytidine deaminases. J. Virol. **80:**605–614.
13. **Doehle, B. P., A. Schafer, H. L. Wiegand, H. P. Bogerd, and B. R. Cullen.** 2005. Differential sensitivity of murine leukemia virus to APOBEC3-mediated inhibition is governed by virion exclusion. J. Virol. **79:**8201–8207.
14. **Esnault, C., O. Heidmann, F. Delebecque, M. Dewannieux, D. Ribet, A. J. Hance, T. Heidmann, and O. Schwartz.** 2005. APOBEC3G cytidine deaminase inhibits retrotransposition of endogenous retroviruses. Nature **433:**430–433.
15. **Hakata, Y., and N. R. Landau.** 2006. Reversed functional organization of mouse and human APOBEC3 cytidine deaminase domains. J. Biol. Chem. **281:**36624–36631.
16. **Harris, R. S., K. N. Bishop, A. M. Sheehy, H. M. Craig, S. K. Petersen-Mahrt, I. N. Watt, I. N., M. S. Neuberger, and M. H. Malim.** 2003. DNA deamination mediates innate immunity to retroviral infection. Cell **113:**803–809.
17. **Hasenkrug, K. J., A. Valenzuela, V. A. Letts, J. Nishio, B. Chesebro, and W. N. Frankel.** 1995. Chromosome mapping of Rfv3, a host resistance gene to Friend murine retrovirus. J. Virol. **69:**2617–2620.
18. **Iwanami, N., A. Niwa, Y. Yasutomi, N. Tabata, and M. Miyazawa.** 2001. Role of natural killer cells in resistance against friend retrovirus-induced leukemia. J. Virol. **75:**3152–3163.
19. **Jern, P., J. P. Stoye, and J. M. Coffin.** 2007. Role of APOBEC3 in genetic diversity among endogenous murine leukemia viruses. PLoS Genet. **3:**2014–2022.
20. **Jin, X., A. Brooks, H. Chen, R. Bennett, R. Reichman, and H. Smith.** 2005. APOBEC3G/CEM15 (hA3G) mRNA levels associate inversely with human immunodeficiency virus viremia. J. Virol. **79:**11513–11516.
21. **Jonsson, S. R., R. S. LaRue, M. D. Stenglein, S. C. Fahrenkrug, V. Andresdottir, and R. S. Harris.** 2007. The restriction of zoonotic PERV transmission by human APOBEC3G. PLoS ONE **2:**e893.
22. **Kabat, D.** 1989. Molecular biology of Friend viral erythroleukemia. Curr. Top. Microbiol. Immunol. **148:**1–42.
23. **Kanari, Y., M. Clerici, H. Abe, H. Kawabata, D. Trabattoni, S. Lo Caputo, F. Mazzotta, H. Fujisawa, A. Niwa, C. Ishihara, Y. A. Takei, and M. Miyazawa.** 2005. Genotypes at chromosome 22q12-13 are associated with HIV-1-exposed but uninfected status in Italians. AIDS **19:**1015–1024.
24. **Kawabata, H., A. Niwa, S. Tsuji-Kawahara, H. Uenishi, N. Iwanami, H. Matsukuma, H. Abe, N. Tabata, H. Matsumura, and M. Miyazawa.** 2006. Peptide-induced immune protection of $CD8^+$ T cell-deficient mice against Friend retrovirus-induced disease. Int. Immunol. **18:**183–198.
25. **Kina, T., K. Ikuta, E. Takayama, K. Wada, A. S. Majumdar, I. L. Weissman, and Y. Katsura.** 2000. The monoclonal antibody TER-119 recognizes a molecule associated with glycophorin A and specifically marks the late stages of murine erythroid lineage. Br. J. Haematol. **109:**280–287.
26. **Liddament, M. T., W. L. Brown, A. J. Schumacher, and R. S. Harris.** 2004. APOBEC3F properties and hypermutation preferences indicate activity against HIV-1 in vivo. Curr. Biol. **14:**1385–1391.
27. **Mangeat, B., P. Turelli, G. Caron, M. Friedli, L. Perrin, and D. Trono.** 2003. Broad antiretroviral defense by human APOBEC3G through lethal editing of nascent reverse transcripts. Nature **424:**99–103.
28. **Mariani, R., D. Chen, B. Schrofelbauer, F. Navarro, R. Konig, B. Bollman, C. Munk, H. Nymark-McMahon, and N. R. Landau.** 2003. Species-specific exclusion of APOBEC3G from HIV-1 virions by Vif. Cell **114:**21–31.
29. **Marin, M., K. M. Rose, S. L. Kozak, and D. Kabat.** 2003. HIV-1 Vif protein binds the editing enzyme APOBEC3G and induces its degradation. Nat. Med. **9:**1398–1403.
30. **Messer, R. J., U. Dittmer, K. E. Peterson, and K. J. Hasenkrug.** 2004. Essential role for virus-neutralizing antibodies in sterilizing immunity against Friend retrovirus infection. Proc. Natl. Acad. Sci. USA **101:**12260–12265.
31. **Mikl, M. C., I. N. Watt, M. Lu, W. Reik, S. L. Davies, M. S. Neuberger, and C. Rada.** 2005. Mice deficient in APOBEC2 and APOBEC3. Mol. Cell. Biol. **25:**7270–7277.
32. **Miyazawa, M.** 2004. Host genes that influence immune and non-immune resistance mechanisms against retroviral infections. Rec. Res. Dev. Immunol. **6:**105–118.
33. **Miyazawa, M., J. Nishio, and B. Chesebro.** 1988. Genetic control of T cell responsiveness to the Friend murine leukemia virus envelope antigen. Identification of class II loci of the H-2 as immune response genes. J. Exp. Med. **168:**1587–1605.
34. **Miyazawa, M., J. Nishio, K. Wehrly, and B. Chesebro.** 1992. Influence of MHC genes on spontaneous recovery from Friend retrovirus-induced leukemia. J. Immunol. **148:**644–647.
35. **Miyazawa, M., J. Nishio, K. Wehrly, C. S. David, and B. Chesebro.** 1992. Spontaneous recovery from Friend retrovirus-induced leukemia. Mapping of the *Rfv-2* gene in the Q/TL region of mouse MHC. J. Immunol. **148:**1964–1967.
36. **Miyazawa, M., S. Tsuji-Kawahara, and Y. Kanari.** 2008. Host genetic factors that control immune responses to retrovirus infections. Vaccine **26:**2981–2996.
37. **Navarro, F., B. Bollman, H. Chen, R. Konig, Q. Yu, K. Chiles, and N. R. Landau.** 2005. Complementary function of the two catalytic domains of APOBEC3G. Virology **333:**374–386.
38. **Newman, E. N., R. K. Holmes, H. M. Craig, K. C. Klein, J. R. Lingappa, M. H. Malim, and A. M. Sheehy.** 2005. Antiviral function of APOBEC3G can be dissected from cytidine deaminase activity. Curr. Biol. **15:**166–170.
39. **Okeoma, C. M., N. Lovsin, B. M. Peterlin, and S. R. Ross.** 2007. APOBEC3 inhibits mouse mammary tumour virus replication in vivo. Nature **445:**927–930.
40. **Robertson, M. N., M. Miyazawa, S. Mori, B. Caughey, L. H. Evans, S. F. Hayes, and B. Chesebro.** 1991. Production of monoclonal antibodies reactive with a denatured form of the Friend murine leukemia virus gp70 envelope protein: use in a focal infectivity assay, immunohistochemical studies, electron microscopy and western blotting. J. Virol. Methods **34:**255–271.
41. **Sawyer, S. L., M. Emerman, and H. S. Malik.** 2004. Ancient adaptive evolution of the primate antiviral DNA-editing enzyme APOBEC3G. PLoS Biol. **2:**e275.
42. **Schrofelbauer, B., Q. Yu, and N. R. Landau.** 2004. New insights into the role of Vif in HIV-1 replication. AIDS Rev. **6:**34–39.
43. **Shindo, K., A. Takaori-Kondo, M. Kobayashi, A. Abudu, K. Fukunaga, and T. Uchiyama.** 2003. The enzymatic activity of CEM15/Apobec-3G is essential for the regulation of the infectivity of HIV-1 virion but not a sole determinant of its antiviral activity. J. Biol. Chem. **278:**44412–44416.
44. **Sitbon, M., B. Sola, L. Evans, J. Nishio, S. F. Hayes, K. Nathanson, C. F. Garon, and B. Chesebro.** 1986. Hemolytic anemia and erythroleukemia, two distinct pathogenic effects of Friend MuLV: mapping of the effects to different regions of the viral genome. Cell **47:**851–859.
45. **Stopak, K., C. de Noronha, W. Yonemoto, and W. C. Greene.** 2003. HIV-1 Vif blocks the antiviral activity of APOBEC3G by impairing both its translation and intracellular stability. Mol. Cell **12:**591–601.
46. **Sugahara, D., S. Tsuji-Kawahara, and M. Miyazawa.** 2004. Identification of a protective $CD4^+$ T-cell epitope in $p15^{gag}$ of Friend murine leukemia virus and role of the MA protein targeting the plasma membrane in immunogenicity. J. Virol. **78:**6322–6334.
47. **Super, H. J., K. J. Hasenkrug, S. Simmons, D. M. Brooks, R. Konzek, K. D. Sarge R. I. Morimoto, N. A. Jenkins, D. J. Gilbert, N. G. Copeland, W. Frankel, and B. Chesebro.** 1999. Fine mapping of the friend retrovirus resistance gene, *Rfv3*, on mouse chromosome 15. J. Virol. **73:**7848–7852.
48. **Tomonaga, K., and J. M. Coffin.** 1999. Structures of endogenous nonecotropic murine leukemia virus (MLV) long terminal repeats in wild mice: implication for evolution of MLVs. J. Virol. **733:**4327–4340.
49. **Yu, X., Y. Yu, B. Liu, K. Luo, W. Kong, P. Mao, and X. F. Yu.** 2003. Induction of APOBEC3G ubiquitination and degradation by an HIV-1 Vif-Cul5-SCF complex. Science **302:**1056–1060.

IL-4/IL-13 antagonist DNA vaccination successfully suppresses Th2 type chronic dermatitis

T. Morioka, K. Yamanaka, H. Mori, Y. Omoto, K. Tokime, M. Kakeda, I. Kurokawa, E.C. Gabazza,* A. Tsubura,† Y. Yasutomi‡ and H. Mizutani

*Department of Dermatology and *Department of Immunology, Mie University, Graduate School of Medicine, 2-174 Edobashi, Tsu, Mie 514-8507, Japan*
†Department of Pathology II, Kansai Medical University, Moriguchi, Osaka 570-8507, Japan
‡Laboratory of Immunoregulation and Vaccine Research, Tsukuba Primate Research Center, National Institute of Biomedical Innovation, Tsukuba, Ibaraki 305-0843, Japan

Summary

Background Atopic dermatitis (AD) is a chronic disease with a Th2-type-cytokine dominant profile. Several cytokines and related peptides have been used for the treatment of AD but they were ineffective because of their limited biological half-life. We have recently developed a highly efficient mouse dominant negative interleukin (IL)-4/IL-13 antagonist (IL-4DM), which blocks both IL-4 and IL-13 signal transductions.

Objective To examine the effects of IL-4DM *in vivo* in an AD model induced by the repeated exhibition of oxazolone (OX).

Methods Plasmid DNA was injected intraperitoneally to cause an experimental AD-like dermatitis. The effect was evaluated by ear thickness, histological findings, and mast cells counts in the inflamed skin. The plasma IgE and histamine levels were measured. Cytokine production in skin and splenocytes were also analysed.

Results Mice treated with control plasmid developed marked dermatitis with mast cells and eosinophil infiltration, and had increased plasma IgE and histamine levels with a Th2 type splenocyte cytokine profile. Treatment with mouse IL-4 DNA augmented the ear swelling and thickness with an increased dermal eosinophil count, plasma histamine level, and production of splenocyte IL-4. However, IL-4DM treatment successfully controlled the dermatitis, decreased the mast cell and eosinophil count, and suppressed plasma IgE and histamine levels. Splenocytes produced an increased level of IFN-γ.

Conclusion These data showed that the simultaneous suppression of IL-4/IL-13 signals successfully controlled Th2-type chronic dermatitis. IL-4DM DNA treatment is a potent therapy for AD and related diseases.

Correspondence
Hitoshi Mizutani.
E-mail: h-mizuta@clin.medic.mie-u.ac.jp

Accepted for publication
17 November 2008

Key words
atopic dermatitis, contact hypersensitivity, DNA vaccine, IL-4 mutant

Conflicts of interest
None declared.

DOI 10.1111/j.1365-2133.2009.09069.x

Interleukin (IL)-4 plays a central role in Th2-cytokine-dominant inflammatory skin diseases such as atopic dermatitis (AD).[1–3] IL-4 is responsible for the differentiation of allergen-specific Th2 cells together with its closely related cytokine IL-13 for the class switching of activated B cells to IgE-producing cells. The effects of IL-13 are similar to IL-4 on B cells, monocytes, and other cell types, but T cells appear to lack an IL-13 binding receptor component and do not respond to IL-13.[4] The structural basis for the overlapping functions of IL-4 and IL-13 is a shared receptor subunit, and IL-4Rα organizes intracellular signals in response to both cytokines.[5,6] Signal transduction is induced by heterodimerization of the IL-4Rα with a second subunit; which may vary according to the cell types. The specific inhibition of IL-4 can be achieved by antagonistic IL-4 mutants. Variants of human IL-4 that bind to the receptor subunit IL-4Rα, but not to the other subunit γ-chain (γc) or IL-13Rα1 are competitive antagonists of IL-4.[7,8] IL-13 is inhibited by similar variants, which form unproductive complexes with IL-4Rα.[5,9] The single-site human IL-4 mutant Y124D has been used as an IL-4/IL-13 inhibitor in various studies,[7–17] but this variant retains some residual agonistic activity, which could be relevant for *in vivo* applications.[7,8] In contrast, IL-4 and IL-13 double mutant R121D/Y124D lacks detectable activity and appears to be an effective antagonist for human IL-4 and IL-13.[5,18]

We have recently developed a highly efficient murine IL-4 antagonist DNA (IL-4DM), in which the amino acids glutamine 116 and tyrosine 119 were changed for aspartic acid.[19] This murine mutant DNA is analogous to the R121D/Y124D double mutant. IL-4DM binds with high affinity to the murine

IL-4Rα without inducing signal transduction, and has no detectable activity upon the proliferation or differentiation of murine cells. An appropriate amount of IL-4DM completely inhibits responses by wild-type IL-4.[19] Like its human analogue, the IL-4DM mutant is also an antagonist of IL-13 (B. Schnarr *et al.*, unpublished data[37]). Recent experiments with monocytes from mice lacking a functional γc gene showed that IL-4DM is a complete inhibitor of IL-4 in the absence of γc as well.[20] In this study we have examined the effects of IL-4DM *in vivo*, using an AD model induced by the repeated exhibition of oxazolone (OX). The repeated application of a hapten such as OX on mice causes an initial delayed-type hypersensitivity that changes to an immediate-type response in the late phase with elevated IgE production and deviation of Th-cell responses. The skin lesions that appear in the late phase are compatible with the clinical findings as well as the cytokine profile observed in AD.[21–23] The inhibitory effect of IL-4DM on IL-4 and IL-13 on the immune response was comparable with that of knockout mice lacking either IL-4[24] or IL-4Rα. Treatment with IL-4DM prevented contact hypersensitivity responses with the increased production of interferon (IFN)-γ.

Materials and methods

Animals

BALB/c male mice aged 5 weeks were purchased from Japan SLC Co. (Shizuoka, Japan) and were used at the age of 6 weeks. Age-matched wild-type BALB/c mice were used as controls. All animals were cared for according to the ethical guidelines approved by the Institutional Animal Care and Use Committee of Mie University.

Reagents

The cDNA coding region of mouse IL-4 was amplified by a polymerase chain reaction (PCR) based on the cDNA sequence of mouse IL-4. The mouse IL-4 fragment was inserted into BamHI and EcoRI-filled in pcDNA3.1+ (Invitrogen, San Diego, CA, U.S.A.) under the TPA leader sequence, and then digested by BamHI and SacI. A Quickchange™ Site-directed Mutagenesis kit (Stratagene, La Jolla, CA, U.S.A.) was used for the mutagenesis of mouse IL-4. The oligonucleotide primers used to prepare a mouse IL-4 double mutant (IL-4DM, Q116D/Y119D) were CTAAAGAGCATCATGGATATGGATGACTCGTAGTCTAGAG and CTCTAGACTACGAGTCATCCATATCCATGATGCTCTTTAG. The IL-4 mutant fragments were ligated into pcDNA3.1+.[25] Mouse IL-4, IL-4DM plasmid DNAs were purified using the Plasmid Mega kit (Qiagen, Chatsworth, CA, U.S.A.) and diluted with sterilized physiological saline. OX was purchased from Sigma (St Louis, MO, U.S.A.) and was dissolved in acetone/olive oil (4 : 1).

Administration of DNA

Mice were treated by intraperitoneal injection of 100 μg of IL-4DM DNA on days 0, 7, 14, 21 and 28. A control plasmid (pcDNA3.1+) vector and IL-4 DNA were also injected on the same day (Fig. 1).

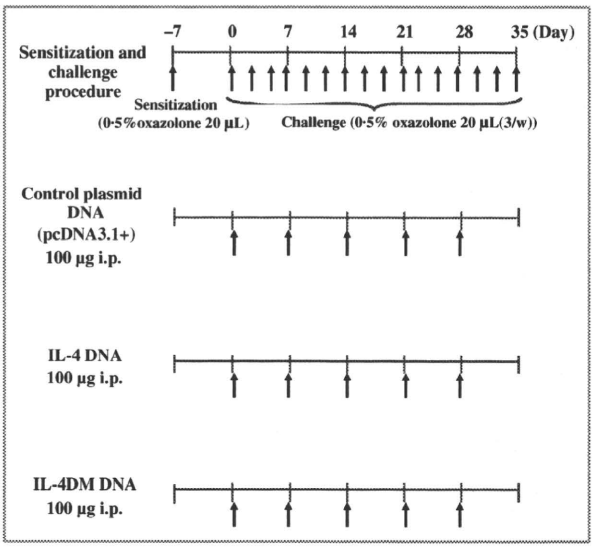

Fig 1. Schedule for induction of chronic contact hypersensitivity and administration of compounds. Mice received intraperitoneal (i.p.) injection of 100 μg of each plasmid DNA on days 0, 7, 14, 21 and 28.

Sensitization and challenge procedures

As shown in Figure 1, mice were initially sensitized by pasting 20 μL of 0·5% OX solution to their left ear 7 days before the first challenge (day 7) and then 20 μL of 0·5% OX solution was repeatedly applied on the left ear three times per week from day 0 as reported previously.[23] Ear swelling was measured with thickness gauge calipers before and 30 min after OX challenge to the pinna of the ear on day 35. The ear swelling response was expressed as the difference between the values taken before and 30 min after application.

Histological analysis

Ear skin specimens obtained 6 h after the final challenge on day 35 were fixed in 10% buffered neutral formaldehyde and embedded in paraffin wax. Histological sections were of 6 μm thickness and they were stained with haematoxylin and eosin. The sections were also stained with 0·5% toluidine blue for the identification of mast cells. The cell counts were performed in six consecutive microscopic fields at × 400 magnification.

Measurement of plasma IgE and plasma histamine

Blood was collected under ether anaesthesia 6 h after the last challenge. Plasma IgE levels were determined by a sandwich enzyme-linked immunosorbent assay (ELISA). In brief, 96-well immunoplates (Corning Inc., Corning, NY, U.S.A.) were coated with 100 μL of an antimouse IgE capture antibody (2 μg mL^{-1}) (BD PharMingen, San Diego, CA, U.S.A.) overnight at 4 °C. Plasma samples of 100 μL were diluted 60-fold with PBS

containing 10% fetal calf serum (FCS) were placed in the wells. After incubation for 1 h at room temperature, 100 μL of biotin-conjugated antimouse IgE antibody (2 μg mL^{-1} in blocking buffer) (BD PharMingen) was added to each well. The plates were incubated at room temperature for 1 h, followed by six washes, incubated with 100 μL of horseradish peroxidase avidin D (FUNAKOSHI, Tokyo, Japan) 1 : 1000 in blocking buffer, and then incubated for 30 min at room temperature. A substrate solution of 100 μL containing 1·5 mg ABTS (Sigma-Aldrich, St Louis, MO, U.S.A.) in 5 mL of a 0·1 mol L^{-1} citric acid solution was added, and kept for 30 min at room temperature in a dark place. Thereafter the reaction was terminated by adding 50 μL of 2 mol L^{-1} H_2SO_4, and the optical density of each well at 405 nm was determined by using a microplate reader. A standard curve was prepared using mouse anti-TNP IgE standard (BD PharMingen). Plasma histamine levels were analysed using the commercial sandwich ELISA kit from Immunoteck (Marseille, France) according to the manufacturer's protocol.

Purification of mRNA from mouse ears

At 6 h after the final challenge, the skin of the left ear was sampled. The specimen was homogenized and the total RNA was extracted using Isogen (Nippon Gene, Tokyo, Japan) according to the manufacturer's instruction; 1 mL of homogenate was vigorously mixed with 200 μL of chloroform, and centrifuged at 12 000 *g* for 15 min at 4 °C. The aqueous phase was separated and mixed with 0·5 mL of 2-propanol (Nacalai Tesque, Kyoto, Japan) to precipitate RNA. After centrifugation, the precipitate was washed with 1 mL of 75% ethanol (Nacalai Tesque) and dried. RNA was suspended in 50 μL of RNase-free water, and the concentration was measured based on the absorbance at 260 nm, and the quality was confirmed by electrophoresis. cDNA was prepared from 10 μg of mRNA using archive kit (ABI, Foster City, CA, U.S.A.) according to the manufacturer's protocol.

Cytokine mRNA expression in skin

The transcriptional activity in the lesional skin samples was measured with a PCR. The amplification of cDNA was performed in 50 μL of a master mixture containing 0·5 μg of cDNA, 200 nmol deoxynucleotide triphosphate, 5 μL of PCR buffer, 2 U of Taq polymerase (ABI) and 2 μmol of each specific primer for the DNA of interest. The following primers were used for PCR reactions (5′–3′), mouse IFN-γ: TCAAGTGGCATAGATGTGGAAGAA and TGGCTCTGCAGGATTTTCATG; mouse IL-2: CCTGAGCAGGATGGAGAATAACA and TCCAGAACATGCCGCAGAG; mouse IL-4: CACTGACGGCACAGAGCTATTGATG and TCATGGTGCAGCTTTCGATGAATC; mouse IL-10: CTCTTACTGACTGGCATGAGGATCAGCAGG and TCTTCACCTGCTCCACTGCCTTGCTCTTAT; mouse IL-12: TCCTGCACTGCTGAAGACATC and TCTCGCCATTATAGATTCAGAGAC; mouse IL-13: AGACCAGACTCCCCTGTGCA and TGGGTCCTGTAGATGGCATTG; mouse β-actin: TGGAATCCTGTGGCATCCATGAAAC and TAAAACGCAGCTCAGTAACAGTCCG.[26] PCR was performed under the following conditions: 95 °C for 5 min, followed by 35 or 40 cycles of 95 °C for 30 s, 56 °C (IFN-γ, IL-12) or 60 °C (IL-2, IL-4, IL-10, IL-13, β-actin) for 30 s, and 72 °C for 1 min were carried out. After the final cycle, the temperature was maintained at 72 °C for 7 min. PCR amplified fragments were electrophoresed through 1·5% agarose gels in tris-acetate EDTA buffer containing ethidium bromide, and the gels were scanned under ultraviolet light. The mRNA of β-actin was used as an internal control. The signal intensity of each reverse transcriptase (RT)-PCR product was estimated using an ATTO Lane & Spot Analyzer (ATTO, Shizuoka, Japan).

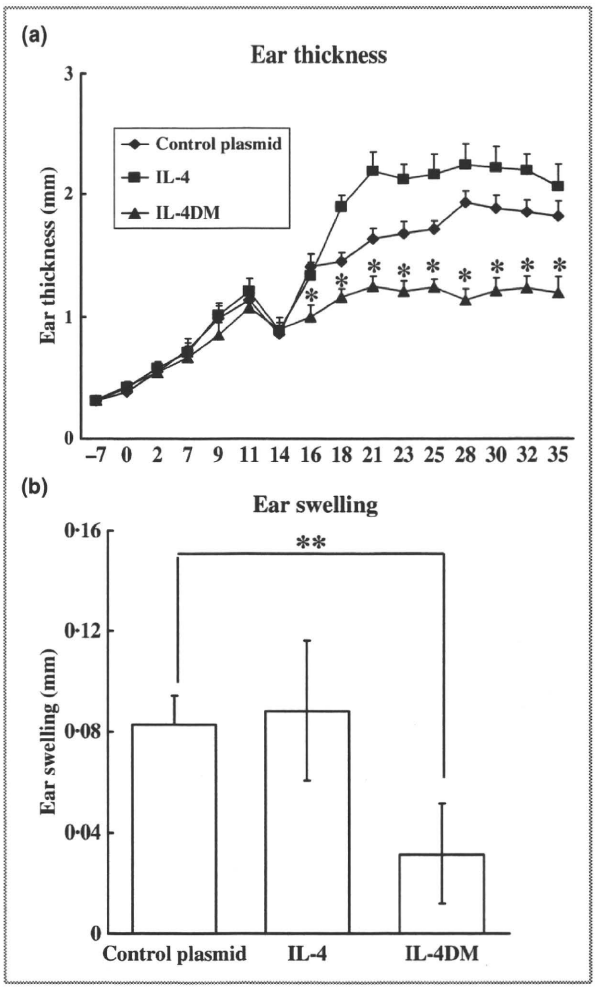

Fig 2. The effects of interleukin (IL)-4DM, IL-4, and control plasmid (pcDNA3.1) on ear swelling induced by repeated application of oxazolone (OX). (a) Ear thickness was measured before each OX challenge. Each point represents the mean ± SD of seven or eight mice. *$P < 0·05$: significantly different from the control group and IL-4 (Student's *t*-test). (b) Inhibition of the effecter phase of chronic hypersensitivity by IL-4DM, IL-4, and control plasmid DNA transfer. The ear swelling was measured 30 min after applying OX. The ear swelling in the IL-4DM groups was significantly suppressed compared with those in the IL-4 and control plasmid DNA groups. *Significant difference from the control by Student's *t*-test at $P < 0·05$.

Cytokine production from splenocytes

A suspension of 2×10^6 splenocytes were made in a solution of 200 μL RPMI-1640 medium (Nikken Bio Medical Laboratory, Kyoto, Japan) containing 10% fetal bovine serum (FBS; Biowest, Nuaillé, France), 50 UI penicillin, 50 μg mL^{-1} streptomycin, and 5 μg mL^{-1} soluble antimouse CD3 (BD Bioscience), and 10 μg mL^{-1} antimouse CD28 (BD Bioscience). Cells were dispensed in triplicate into 96-well flat-bottomed microplates (Sumitomo Bakelite, Tokyo, Japan). After incubation for 48 h at 37 °C in a humidified incubator (5% CO_2), culture supernatants were collected and analysed for IFN-γ (Quantikine; R&D Systems, Minneapolis, MN, U.S.A.) or IL-4 (Quantikine; R&D Systems) production with an ELISA according to the manufacturer's protocol.

Statistical analysis

Statistical analysis was performed using Student's t-test and Mann–Whitney U-test. Values are expressed as mean ± SEM. A 95% confidence limit was taken as significant ($P < 0.05$).

Result

Ear thickness with the treatment of IL-4DM, IL-4, or control plasmid

In the control group, the ear thickness increased from the beginning of the challenge, and increased gradually through the experiments (Fig. 2a). The agonistic IL-4 DNA treatment augmented increase of the ear thickness after day 16. In contrast, IL-4DM DNA treatment significantly suppressed increase of the ear thickness compared with that of control plasmid or IL-4DNA-treated mice.

Effects of IL-4DM on the oxazolone-induced acute-phase ear swelling

The ear swelling was also measured 30 min after OX application on day 35, and the difference between before and 30 min after application was calculated. IL-4DM DNA treatment suppressed the ear swelling significantly compared with that of the control DNA-injected group (Fig. 2b). However, IL-4DNA showed no suppressive effects.

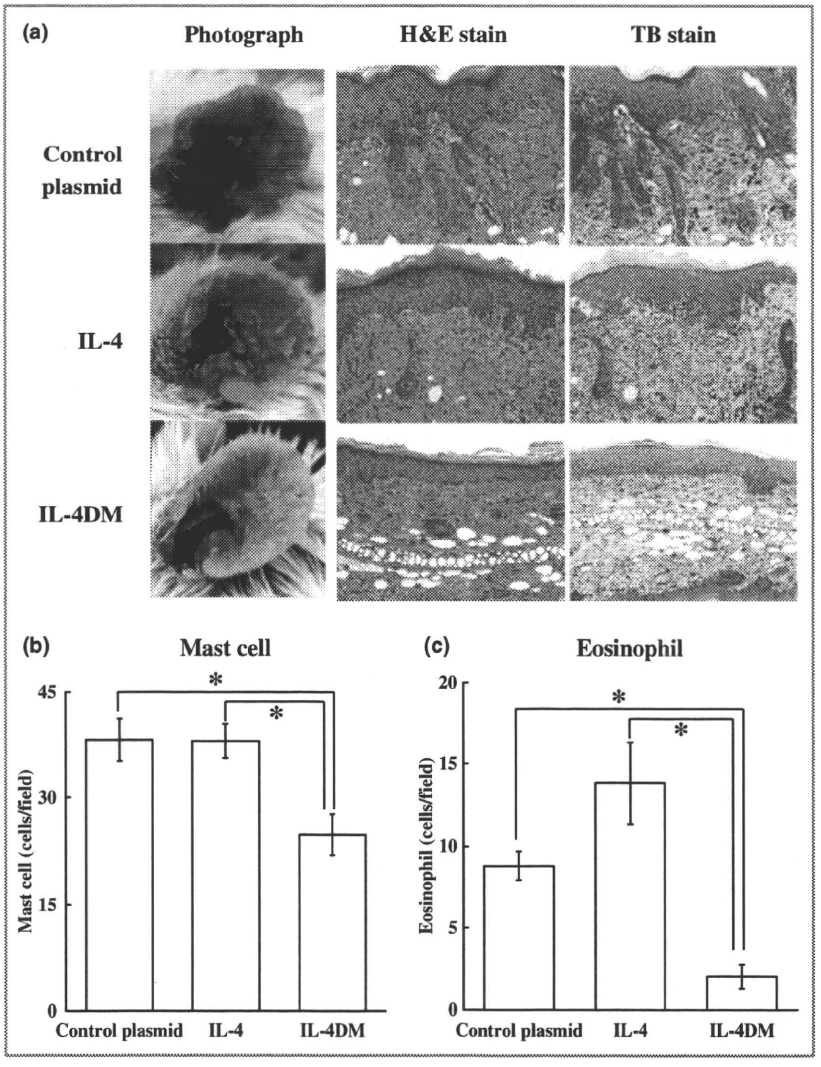

Fig 3. (a) Representative photographs and histological feature of oxazolone (OX)-treated skin lesion. OX-sensitized ear revealed hyperkeratosis, acanthosis, and parakeratosis in control and interleukin (IL)-4-treated mice. An increased number of infiltrating lymphocytes, macrophages and mast cells was observed in the skin lesions, all of which are typical histological findings observed in patients with atopic dermatitis. In contrast, acanthosis was clearly suppressed, and skin infiltration of granulocytes, eosinophils, and mast cells was decreased in the IL-4DM-treated mice as compared with control plasmid-treated mice (original magnification × 200). (b) The number of dermal mast cells was counted, and found to be decreased in the IL-4DM-treated mice. (c) The number of dermal eosinophils was also counted in 10 high power fields. The skin infiltration of eosinophils was significantly decreased in the IL-4DM-treated mice. Data are expressed as the mean ± SEM. *Significant difference by Student's t-test at $P < 0.05$.

Histological findings and mast cell counts in the inflamed skin

In control plasmid-treated mice and IL-4 DNA-treated mice, severe dermatitis was observed on the earlobe. A drastic decrease of inflammation was observed in IL-4DM DNA-treated mice (Fig. 3a). Histological examination on the OX-challenged ear skin revealed hyperkeratosis, acanthosis and parakeratosis in both of the control and IL-4-treated mice. An increased number of infiltrating lymphocytes, macrophages and mast cells was observed in the skin lesions in control DNA and IL-4 DNA-treated mice. These findings are comparable with those of AD skin lesions. In contrast, the acanthotic changes and infiltration of granulocytes, mast cells, and eosinophils were significantly suppressed in the IL-4DM DNA-treated mice compared with those of control DNA- or IL-4 DNA-treated mice (Fig. 3b,c). Interestingly, IL-4 DNA treatment increased eosinophil counts compared with control DNA treatment.

Plasma IgE and histamine levels

The total plasma IgE level was increased by repeated OX challenges (Fig. 4a). IL-4 DNA treatment showed no agonistic effects in the plasma IgE level; however, IL-4DM DNA treatment significantly suppressed the levels of plasma IgE. The plasma histamine level was also significantly increased in the control DNA- or IL-4 DNA-treated mice; however, IL-4DM DNA treatment significantly suppressed the plasma histamine levels (Fig. 4b).

Cytokine mRNA expression levels

To determine the effects of IL-4DM on cytokine production in the inflamed skin lesions, mRNA expression of Th1 and Th2 cytokines was analysed. The IFN-γ mRNA expression was significantly increased in IL-4DM DNA-treated mice ear compared with that of control DNA-treated samples (standardized by β-actin expression).

However, no remarkable difference in other cytokine mRNA expression was observed among three different DNA-treated samples (Fig. 5a,b).

Concentration of IFN-γ and IL-4 in splenocyte cell culture supernatants

To know the effects of IL-4DM DNA therapy in the systemic immune system, the concentration of IFN-γ in splenocyte cell culture supernatants was measured by ELISA. The IFN-γ level in the IL-4DM-treated samples was significantly higher than that in the control DNA- or IL-4 DNA-treated samples (Fig. 6a). We also measured the concentration of IL-4 in splenocyte cell culture supernatants by ELISA for mouse IL-4. The IL-4 level in the IL-4DM-treated samples was as high as the IL-4 DNA-treated samples. These were higher than that of the control DNA-treated samples (Fig. 6b).

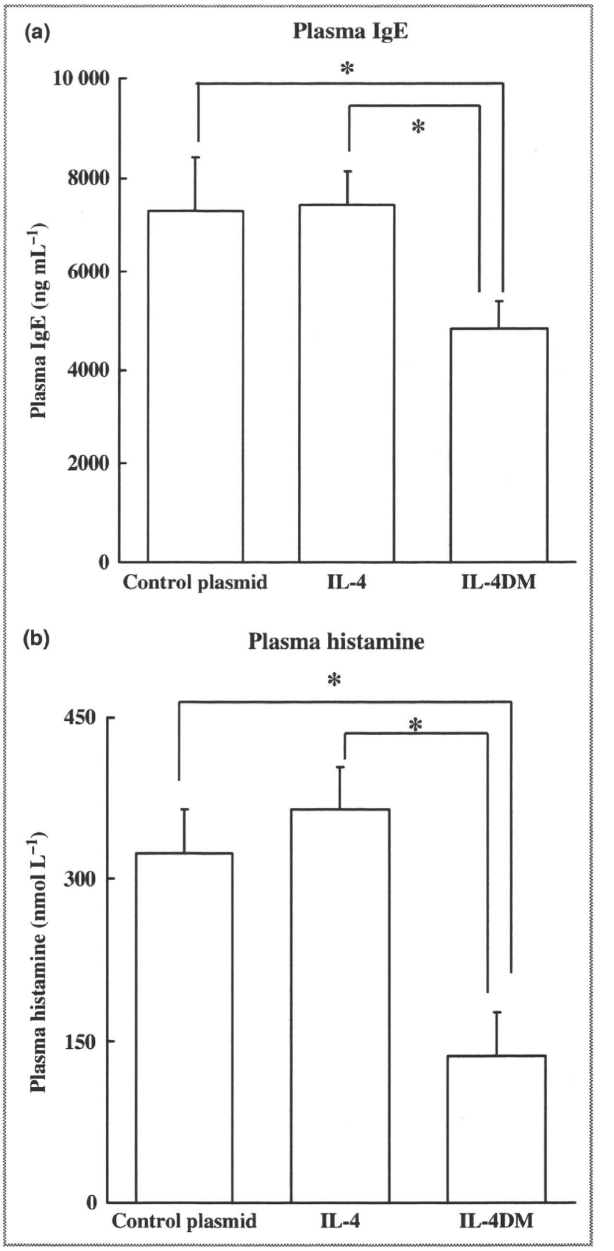

Fig 4. Plasma IgE and histamine levels. (a) Plasma IgE level was decreased in interleukin (IL)-4DM treated mice. (b) Inhibition of the production of plasma histamine was observed in IL-4DM DNA-treated mice. *Significant difference from the IL-4 and control by Mann–Whitney U-test at $P < 0{\cdot}05$.

Discussion

Several previous studies have shown that AD is a chronic dermatitis with a predominance of Th2 cytokines in the lesional skin,[27–29] and that Th2 cytokines play a critical role in the pathogenesis of dermatitis.[28] IL-4 is one of the Th2 cytokines that affects the function of different cell types including T cells, B cells, mast cells, monocytes/macrophages, endothelial cells, fibroblasts, dendritic cells, Langerhans cells

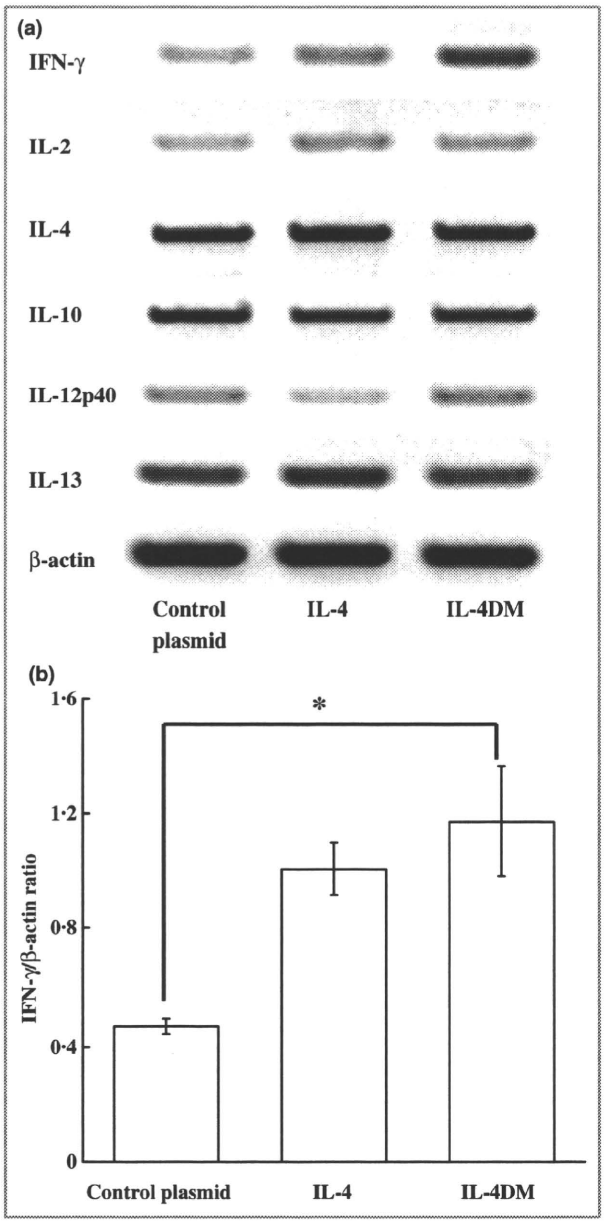

Fig 5. (a) Reverse-transcriptase polymerase chain reaction analysis of cytokine mRNA expression 6 h after oxazolone (OX)-sensitization. The cDNAs were amplified for respective cycles of six cytokines and β-actin, subjected to electrophoresis, and visualized with ethidium bromide. Representative results under optimal conditions are shown. Although almost all Th1 and Th2 cytokine levels were unchanged, mRNA expression for interferon (IFN)-γ was increased in IL-4DM-treated mice. (b) The level of mRNA expression of IFN-γ was expressed as the value relative to that for β-actin. The IFN-γ level in the IL-4DM group is significantly higher than that of control plasmid groups. *Significant difference from the control by Student's t-test at $P < 0{\cdot}05$.

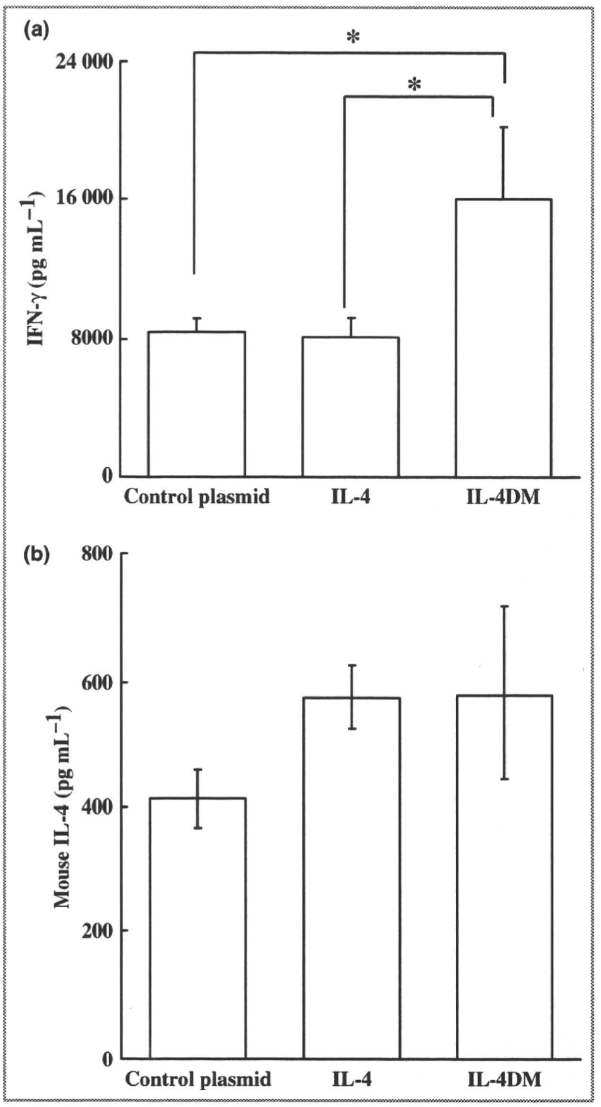

Fig 6. Cytokine production from splenocytes in chronic hypersensitivity mice. Interferon (IFN)-γ and interleukin (IL)-4 production from splenocytes was measured. (a) Actual IFN-γ protein production was increased in the IL-4DM-treated mice. (b) IL-4 levels did not reach the significance, but showed a tendency to increase in the IL-4 and IL-4DM mice. *Significant difference from the control by Mann–Whitney *U*-test at $P < 0{\cdot}05$.

and keratinocytes. Because of this broad-spectrum action, IL-4 is believed to play a crucial role in the pathogenesis of AD.[30,31] In the present study, we employed a contact hypersensitivity model by the repeated application of OX, which mimics the histological phenotype of AD in humans; this model also showed increased levels of Th2 cytokines in the lesional skin as reported by Kitagaki *et al.*[21]

Immunotherapy such as the direct blocking of Th2 responses with neutralizing antibody against Th2 cytokines, the soluble form of IL-4 receptor (IL-4R), or antagonistic IL-4 mutant proteins have been used for the treatment of asthma.[32–34] These proteins directly inhibit IL-4 binding thereby inhibiting host immune responses. A previous study by Nishikubo *et al.*[25] showed inhibition of immune responses by using IL-4 mutant protein for at least 50 weeks. However, results from these experimental animals have shown that the application of these trials to humans is difficult. Because the pharmacokinetic half-life of IL-4 mutant and sIL-4R protein

are very short in *vivo* (IL-4 mutant: $t_{1/2}$ = 0·83 h; sIL-4R: $t_{1/2}$ = 4·6 h),[35,36] huge amounts of these molecules are required in plasma to maintain a long period of inhibitory action on allergic inflammation. In fact, administration of these molecules was required many times in high doses from the sensitization to the challenge periods.[35–37] In the present study, we demonstrated a remarkable antagonistic effect of IL-4 mutant DNA applied in a form of vaccination, as a potent new type of immunogene therapy for AD. In previous studies in which gene therapy and DNA vaccines were used in combination with a cytokine gene for tumours or pathogens, effective immune responses to antigen were recognized even in the absence of detectable plasma levels of cytokines. Recently, we also reported that administration of plasmid DNA coding IL-4 cDNA completely inhibited the development of insulitis, which is one of the Th1-type autoimmune diseases, although no IL-4 was detected in plasma.[38] These results suggest that genes applied as a DNA vaccine express and supply products to the host continuously. To occupy the IL-4/IL-13 receptors, a continuous supply of IL-4DM is needed but not bolus application. Therefore, IL-4DM applied as a DNA vaccine might inhibit the allergic inflammation by persistent secretion of mutant IL-4 over a long period in a limited amount.

As we had expected, IL-4DM mitigated phenotypical and histological changes such as severe oedema, inflammatory cell infiltration and epidermal hyperplasia. IL-4DM also significantly decreased the number of dermal mast cells. IL-4 is known to be a potent activator of mast cells. Mast cells, which participate in the inflammatory cascade, serve as an abundant source of Th2 cytokines as well as inflammatory mediators.[39–41] Therefore, inhibition of mast cell activation is another possible mechanism through which IL-4DM ameliorates inflammatory responses in the present model of dermatitis. Eosinophil infiltration into the dermis has been well documented in AD.[42] In this study, an increased number of eosinophils was observed in contact hypersensitivity skin lesions, and was dramatically inhibited by IL-4DM treatment. Inhibition of cellular infiltration in IL-4DM mice may be due to suppression of IL-4-mediated immunological events such as a decreased expression of cellular adhesion molecules on endothelial cells.[43]

Injected IL-4DM and IL-4 DNA are trapped by monocytes/macrophages by phagocytosis. They may migrate to lymph nodes or spleen and show systemic effects. In fact, we could observe a high concentration of IL-4 in cultured splenocytes from IL-4DM DNA injected mice by ELISA. Unfortunately, there is no specific anti-IL-4DM antibody or anti-IL-4DM ELISA. The standard ELISA used in this study could not differentiate the natural mouse IL-4 and mutant IL-4 protein; these findings are consistent with the previous report.[25] The plasma IL-4 levels in the agonistic IL-4DNA-treated mice were consistent with those of the IL-4DM DNA-treated mice. Therefore, we speculate that exogenously applied IL-4DM DNAs were expressed the same as IL-4 DNAs, and showed systemic immunological effects.

IFN-γ production increased systemically and locally in mice treated with IL-4DM DNA. Repeated OX treatments cause expansion both of Th1 and Th2 cells. IL-4DM DNA therapy interfered with the development of the Th2 milieu. Subsequently, IFN-γ production and mRNA expression might become abundant locally and systemically.

Tissue-specific gene transfer could be achieved naturally and effectively through the cell specificity of virus receptors.[44] However, there may be a risk of vector toxicity through viral infection of host cells. Also, the limited size of transgenes is often a serious obstacle. Moreover, immune responses to viral vectors are also induced, and the effects of transgenes are eliminated by immune responses to the vectors. For human applications, the efficacy and safety of any delivery system for gene transfer are always of major concern. Nonviral approaches are advantageous in immunogene therapy. DNA vaccines are capable of inducing potent biological effects in a variety of experimental systems.[45] One of the characteristic features of DNA vaccines is their ability to induce long-lasting immunity. The animals that had been treated with IL-4DM DNA did not develop severe allergic inflammation even before or after antigen sensitization.

In the present study, we showed the beneficial effects of immunogene therapy with IL-4 mutant DNA in an experimental model for AD. An IL-4 mutant DNA vaccination is a potent new tool for the systemic treatment of AD.

Acknowledgments

Grants-in-Aid for Scientific Research and Grants-in-Aid for Core Research Evolutional Science and Technology.

References

1 Paul WE. Interleukin-4: a prototypic immunoregulatory lymphokine. *Blood* 1991; **77**:1859–70.
2 Mosmann TR, Sad S. The expanding universe of T-cell subsets: Th1, Th2 and more. *Immunol Today* 1996; **17**:138–46.
3 Romagnani S. The Th1/Th2 paradigm. *Immunol Today* 1997; **18**:263–6.
4 Zurawski G, de Vries JE. Interleukin 13, an interleukin 4-like cytokine that acts on monocytes and B cells, but not on T cells. *Immunol Today* 1994; **15**:19–26.
5 Tony HP, Shen BJ, Reusch P *et al.* Design of human interleukin-4 antagonists inhibiting interleukin-4-dependent and interleukin-13-dependent responses in T-cells and B-cells with high efficiency. *Eur J Biochem* 1994; **225**:659–65.
6 Smerz-Bertling C, Duschl A. Both interleukin 4 and interleukin 13 induce tyrosine phosphorylation of the 140-kDa subunit of the interleukin 4 receptor. *J Biol Chem* 1995; **270**:966–70.
7 Kruse N, Tony HP, Sebald W. Conversion of human interleukin-4 into a high affinity antagonist by a single amino acid replacement. *EMBO J* 1992; **11**:3237–44.
8 Kruse N, Shen BJ, Arnold S *et al.* Two distinct functional sites of human interleukin 4 are identified by variants impaired in either receptor binding or receptor activation. *EMBO J* 1993; **12**:5121–9.
9 Zurawski SM, Vega F Jr, Huyghe B *et al.* Receptors for interleukin-13 and interleukin-4 are complex and share a novel component that functions in signal transduction. *EMBO J* 1993; **12**:2663–70.

10 Aversa G, Punnonen J, Cocks BG *et al.* An interleukin 4 (IL-4) mutant protein inhibits both IL-4 or IL-13-induced human immunoglobulin G4 (IgG4) and IgE synthesis and B cell proliferation: support for a common component shared by IL-4 and IL-13 receptors. *J Exp Med* 1993; **178**:2213–18.

11 Zurawski SM, Chomarat P, Djossou O *et al.* The primary binding subunit of the human interleukin-4 receptor is also a component of the interleukin-13 receptor. *J Biol Chem* 1995; **270**:13869–78.

12 Konig B, Fischer A, Konig W. Modulation of cell-bound and soluble CD23, spontaneous and ongoing IgE synthesis of human peripheral blood mononuclear cells by soluble IL-4 receptors and the partial antagonistic IL-4 mutant protein IL-4 (Y124D). *Immunology* 1995; **85**:604–10.

13 Carballido JM, Schols D, Namikawa R *et al.* IL-4 induces human B cell maturation and IgE synthesis in SCID-hu mice. Inhibition of ongoing IgE production by *in vivo* treatment with an IL-4/IL-13 receptor antagonist. *J Immunol* 1995; **155**:4162–70.

14 Carballido JM, Aversa G, Schols D *et al.* Inhibition of human IgE synthesis *in vitro* and in SCID-hu mice by an interleukin-4 receptor antagonist. *Int Arch Allergy Immunol* 1995; **107**:304–7.

15 Schnyder B, Lugli S, Feng N *et al.* Interleukin-4 (IL-4) and IL-13 bind to a shared heterodimeric complex on endothelial cells mediating vascular cell adhesion molecule-1 induction in the absence of the common gamma chain. *Blood* 1996; **87**:4286–95.

16 Sornasse T, Larenas PV, Davis KA *et al.* Differentiation and stability of T helper 1 and 2 cells derived from naive human neonatal CD4+ T cells, analyzed at the single-cell level. *J Exp Med* 1996; **184**:473–83.

17 Vannier E, de Waal Malefyt R, Salazar-Montes A *et al.* Interleukin-13 (IL-13) induces IL-1 receptor antagonist gene expression and protein synthesis in peripheral blood mononuclear cells: inhibition by an IL-4 mutant protein. *Blood* 1996; **87**:3307–15.

18 Schnarr B, Ezernieks J, Sebald W *et al.* IL-4 receptor complexes containing or lacking the gamma C chain are inhibited by an overlapping set of antagonistic IL-4 mutant proteins. *Int Immunol* 1997; **9**:861–8.

19 Grunewald SM, Kunzmann S, Schnarr B *et al.* A murine interleukin-4 antagonistic mutant protein completely inhibits interleukin-4-induced cell proliferation, differentiation, and signal transduction. *J Biol Chem* 1997; **272**:1480–3.

20 Andersson A, Grunewald SM, Duschl A *et al.* Mouse macrophage development in the absence of the common gamma chain: defining receptor complexes responsible for IL-4 and IL-13 signaling. *Eur J Immunol* 1997; **27**:1762–8.

21 Kitagaki H, Fujisawa S, Watanabe K *et al.* Immediate-type hypersensitivity response followed by a late reaction is induced by repeated epicutaneous application of contact sensitizing agents in mice. *J Invest Dermatol* 1995; **105**:749–55.

22 Kitagaki H, Kimishima M, Teraki Y *et al.* Distinct *in vivo* and *in vitro* cytokine profiles of draining lymph node cells in acute and chronic phases of contact hypersensitivity: importance of a type 2 cytokine-rich cutaneous milieu for the development of an early-type response in the chronic phase. *J Immunol* 1999; **163**:1265–73.

23 Mori H, Yamanaka K, Matsuo K *et al.* Administration of Ag85B showed therapeutic effects to Th2-type cytokine-mediated acute phase atopic dermatitis by inducing regulatory T cells. *Arch Dermatol Res* 2009; **301**:151–7.

24 Kopf M, Le Gros G, Bachmann M *et al.* Disruption of the murine IL-4 gene blocks Th2 cytokine responses. *Nature* 1993; **362**:245–8.

25 Nishikubo K, Murata Y, Tamaki S *et al.* A single administration of interleukin-4 antagonistic mutant DNA inhibits allergic airway inflammation in a mouse model of asthma. *Gene Ther* 2003; **10**:2119–25.

26 Overbergh L, Valckx D, Waer M *et al.* Quantification of murine cytokine mRNAs using real time quantitative reverse transcriptase PCR. *Cytokine* 1999; **11**:305–12.

27 Kay AB, Ying S, Varney V *et al.* Messenger RNA expression of the cytokine gene cluster, interleukin 3 (IL-3), IL-4, IL-5, and granulocyte/macrophage colony-stimulating factor, in allergen-induced late-phase cutaneous reactions in atopic subjects. *J Exp Med* 1991; **173**:775–8.

28 Herz U, Bunikowski R, Renz H. Role of T cells in atopic dermatitis. New aspects on the dynamics of cytokine production and the contribution of bacterial superantigens. *Int Arch Allergy Immunol* 1998; **115**:179–90.

29 Akdis CA, Akdis M, Trautmann A *et al.* Immune regulation in atopic dermatitis. *Curr Opin Immunol* 2000; **12**:641–6.

30 Ricci M, Matucci A, Rossi O. IL-4 as a key factor influencing the development of allergen-specific Th2-like cells in atopic individuals. *J Investig Allergol Clin Immunol* 1997; **7**:144–50.

31 Elbe-Burger A, Egyed A, Olt S *et al.* Overexpression of IL-4 alters the homeostasis in the skin. *J Invest Dermatol* 2002; **118**:767–78.

32 Zhou CY, Crocker IC, Koenig G *et al.* Anti-interleukin-4 inhibits immunoglobulin E production in a murine model of atopic asthma. *J Asthma* 1997; **34**:195–201.

33 Tomaki M, Zhao LL, Lundahl J *et al.* Eosinophilopoiesis in a murine model of allergic airway eosinophilia: involvement of bone marrow IL-5 and IL-5 receptor alpha. *J Immunol* 2000; **165**:4040–50.

34 Bost KL, Holton RH, Cain TK *et al.* *In vivo* treatment with anti-interleukin-13 antibodies significantly reduces the humoral immune response against an oral immunogen in mice. *Immunology* 1996; **87**:633–41.

35 Henderson WR Jr, Chi EY, Maliszewski CR. Soluble IL-4 receptor inhibits airway inflammation following allergen challenge in a mouse model of asthma. *J Immunol* 2000; **164**:1086–95.

36 Tomkinson A, Duez C, Cieslewicz G *et al.* A murine IL-4 receptor antagonist that inhibits IL-4- and IL-13-induced responses prevents antigen-induced airway eosinophilia and airway hyperresponsiveness. *J Immunol* 2001; **166**:5792–800.

37 Grunewald SM, Werthmann A, Schnarr B *et al.* An antagonistic IL-4 mutant prevents type I allergy in the mouse: inhibition of the IL-4/IL-13 receptor system completely abrogates humoral immune response to allergen and development of allergic symptoms *in vivo*. *J Immunol* 1998; **160**:4004–9.

38 Hayashi T, Yasutomi Y, Hasegawa K *et al.* Interleukin-4-expressing plasmid DNA inhibits reovirus type-2-triggered autoimmune insulitis in DBA/1 J suckling mice. *Int J Exp Pathol* 2003; **84**:101–6.

39 Ruzicka T, Gluck S. Cutaneous histamine levels and histamine releasability from the skin in atopic dermatitis and hyper-IgE-syndrome. *Arch Dermatol Res* 1983; **275**:41–4.

40 Horsmanheimo L, Harvima IT, Jarvikallio A *et al.* Mast cells are one major source of interleukin-4 in atopic dermatitis. *Br J Dermatol* 1994; **131**:348–53.

41 Gibbs BF, Wierecky J, Welker P *et al.* Human skin mast cells rapidly release preformed and newly generated TNF-alpha and IL-8 following stimulation with anti-IgE and other secretagogues. *Exp Dermatol* 2001; **10**:312–20.

42 Leung DY. Atopic dermatitis: immunobiology and treatment with immune modulators. *Clin Exp Immunol* 1997; **107** (Suppl. 1):25–30.

43 Schleimer RP, Sterbinsky SA, Kaiser J *et al.* IL-4 induces adherence of human eosinophils and basophils but not neutrophils to endothelium. Association with expression of VCAM-1. *J Immunol* 1992; **148**:1086–92.

44 Mistry AR, Falciola L, Monaco L *et al.* Recombinant HMG1 protein produced in Pichia pastoris: a nonviral gene delivery agent. *BioTechniques* 1997; **22**:718–29.

45 Gurunathan S, Klinman DM, Seder RA. DNA vaccines: immunology, application, and optimization. *Annu Rev Immunol* 2000; **18**:927–74.

Arch Dermatol Res
DOI 10.1007/s00403-008-0873-y

ORIGINAL PAPER

Administration of Ag85B showed therapeutic effects to Th2-type cytokine-mediated acute phase atopic dermatitis by inducing regulatory T cells

Hitoshi Mori · Keiichi Yamanaka · Kazuhiro Matsuo · Ichiro Kurokawa · Yasuhiro Yasutomi · Hitoshi Mizutani

Received: 5 February 2008 / Revised: 22 May 2008 / Accepted: 20 June 2008

Abstract Increase in the number of patients with atopic dermatitis (AD) has been recently reported. T helper (Th) cells that infiltrate AD skin lesions are Th2-type dominant; reduced exposure to environmental Th1-cytokine-inducing microbes is believed to contribute to the increased number of AD patients. Regulatory type immune responses have been also associated with the occurrence of AD. It has been reported that antigen 85B (Ag85B) purified from mycobacteria is a potent inducer of Th1-type immune response in mice as well as in humans. In this study, we have examined the effect of plasmid DNA encoding Ag85B derived from *Mycobacterium kansasii* on AD skin lesions induced by oxazolone (OX) application. Th2-cytokine mediated mouse AD model with immediate type response followed by a late phase reaction was developed by repeated applications of low-dose OX to sensitized mice. Mice were immunized with plasmid DNA encoding cDNA of Ag85B before OX sensitization or during repeated elicitation phase. Both therapies were associated with significant suppression of immediate type response, clinical appearance, dermal cell infiltration, reduced IL-4 production, and augmented IFN-γ mRNA expression compared to placebo-treated mice. Additionally, increased number of Foxp3$^+$ regulatory T cells were observed in the skin sections in Ag85B treated mice. The results of this study suggest that Ag85B DNA vaccine is a potential therapy for Th2 type dermatitis.

Keywords Atopic dermatitis · Antigen 85B · Regulatory T cell

Abbreviations

AD	Atopic dermatitis
Th	T helper
BCG	*Bacillus Calmette-Güerin*
Treg	Regulatory T cell
Ag85B	Antigen 85B
OX	Oxazolone

Introduction

It is known that acute phase skin lesion in atopic dermatitis (AD) is associated with enhanced secretion of T helper (Th) 2-type cytokines [8]. Increased incidence of atopic disorders has been reported in industrialized countries; according to the hygiene hypothesis, the increase in the incidence of patients may be explained by a better lifestyle and less exposure to environmental microbes [5, 7, 28]. Environmental microbes such as mycobacteria or certain virus may promote Th1-type immune response and thus reducing atopy-associated Th2-type reaction. For instance, the study

H. Mori · K. Yamanaka · I. Kurokawa · H. Mizutani (✉)
Department of Dermatology,
Mie University Graduate School of Medicine,
2-174 Edobashi, Tsu, Mie 514-8507, Japan
e-mail: h-mizuta@clin.medic.mie-u.ac.jp

K. Matsuo
Research and Development Department,
Japan BCG Laboratory, Tokyo, Japan

Y. Yasutomi
Laboratory of Immunoregulation and Vaccine Research,
Tsukuba Primate Research Center,
National Institute of Biomedical Innovation,
Tsukuba, Ibaraki, Japan

Y. Yasutomi
Department of Immunoregulation,
Mie University Graduate School of Medicine,
Tsu, Mie, Japan